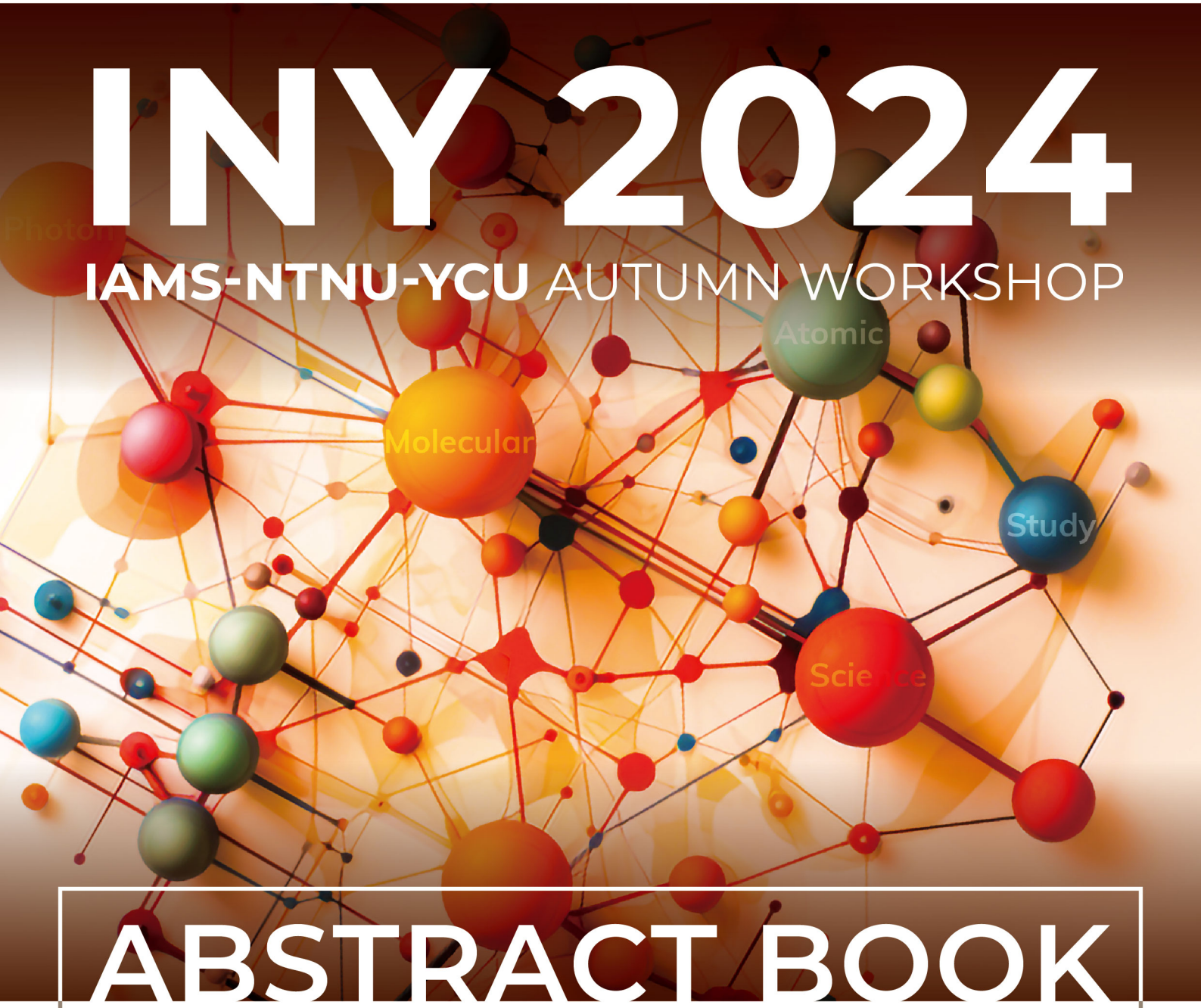

INY 2024

IAMS-NTNU-YCU AUTUMN WORKSHOP

ABSTRACT BOOK

AUGUST 26

2024

中央研究院 原子與分子科學研究所
Institute of Atomic and Molecular Sciences
Academia Sinica

國立臺灣師範大學
NATIONAL TAIWAN NORMAL UNIVERSITY

YOKOHAMA CITY UNIVERSITY

INY 2024 IAMS-NTNU-YCU AUTUMN WORKSHOP 2024

中央研究院 原子與分子科學研究所 Institute of Atomic and Molecular Sciences Academia Sinica | 國立臺灣師範大學 NATIONAL TAIWAN NORMAL UNIVERSITY | YOKOHAMA CITY UNIVERSITY

Date August 26

Program

08:50 ~ 09:20	**Registration**
09:20 ~ 09:30	**Opening Remarks** IAMS side: Director Dr. Ching-Ming Wei (IAMS) | NTNU side: Prof. Ting-Hua Lu (NTNU)
	Session A Chair : Prof. Ting-Hua Lu (NTNU)
09:30 ~ 09:45	**Fizza Sabbor (IAMS)** Stereoselectivity in Matching Partners: Navigating the Influence of Reaction Parameters in Glycosylation
09:45 ~ 10:00	**Ayune Mizukami (YCU)** Mechanical properties of C60 nanowhiskers after heat treatment
10:00 ~ 10:15	**Suguru Ushioda (YCU)** Will clathrin coated pits be always spherical?
10:15 ~ 10:30	**Chia-Hsiang Chuang (NTNU)** Characteristics in 1D & 2D chiral perovskite single crystals and thin films
10:30 ~ 10:50	**Coffee Break & Group Photo**
	Session B Chair : Prof. Tomomi Shimazaki (YCU)
10:50 ~ 11:05	**I Gusti Ngurah Yudi Handayana (IAMS)** Atomic excitation trapping in dissimilar atomic array with chiral coupling
11:05 ~ 11:20	**Yan-Ru Chu (NTNU)** Hydrogenation Effect on Antisymmetric Magnetoresistance in Co/Pd Multilayers
11:20 ~ 11:35	**Suraj Singh (IAMS)** Uniform Growth and Characterization of Hexagonal Boron Nitride (h-BN) on Dielectric Substrates for Quantum Technology Applications
11:35 ~ 11:50	**Shih-Po Chien (NTNU)** Probing Phonon Symmetry Breaking in MoS2 Using Polarized Raman Spectroscopy
11:50 ~ 12:05	**Kentaro Numata (YCU)** Theoretical analysis of positronic compounds of fluorine molecular dianions using quantum Monte Carlo method
12:05 ~ 13:00	**Lunch**
13:00 ~ 14:00	**Poster Session**
14:00 ~ 14:20	**Break (Clean Up Poster Boards)**
	Session C Chair : Prof. Ryo Suzuki (YCU)
14:20 ~ 14:35	**Kotaro Oikawa (YCU)** Correlated photoluminescence blinking phenomenon on InGaN/GaN NanoPillars structures
14:35 ~ 14:50	**Che-Wei Chang (IAMS)** Absolute Line Strength and Rovibrational Spectrum of Hydroperoxyl Radical in the v3 Fundamental Band
14:50 ~ 15:05	**Miina Suzuki (YCU)** Morphology control of protein crystals by hydrogel
15:05 ~ 15:20	**Mio Takakuwa (YCU)** Computational study on the role of residues near the chromophore in Enhanced Green Fluorescent Protein
15:20 ~ 15:40	**Coffee Break**
	Session D Chair : Prof. Jyh-Shen Tsay (NTNU)
15:40 ~ 15:55	**Lily Maysari Angraini (IAMS)** Exploring the influence of S/Cl sites' mixing on the lithium diffusion behaviors of Lix+6PS5Cl
15:55 ~ 16:10	**Pei-Hsuan Lo (NTNU)** Optoelectronic Properties of Chiral NEA Quasi-2D Perovskite Films with Different Precursor Ratios
16:10 ~ 16:25	**Khalil ur Rehman (IAMS)** A magnetic micro-actuator based on particle jamming
16:25 ~ 16:40	**Ye-Ru Chen (NTNU)** Utilizing Light's Orbital Angular Momentum to Boost Photocurrent in MoS2 Transistors
16:40 ~ 16:55	**Yu-Chen Chang (NTNU)** Exploring Exciton-Phonon Interactions in Photoexcited MoS2 by Polarized Raman Spectroscopy
16:55 ~ 17:10	**Break**
17:10 ~ 17:30	**Closing Remarks by Prof. Ryo Suzuki (YCU)** **Award Ceremony by Dr. Tsyr-Yan Dharma Yu (IAMS)**
18:00	**Banquet at 曉鹿鳴樓**

INY IAMS-NTNU-YCU 2024 AUTUMN WORKSHOP 2024

中央研究院 原子與分子科學研究所 Institute of Atomic and Molecular Sciences Academia Sinica | 國立臺灣師範大學 NATIONAL TAIWAN NORMAL UNIVERSITY | YOKOHAMA CITY UNIVERSITY

Date August 26

List of Poster Presentations

No.	Name	Poster Title
1	Chimdessa Gashu Feyisa	Fast generation of multipartite entanglement in non-Hermitian qubits
2	Go Fujihara	Theoretical study on dissociation reaction of nitrogen molecules on lithium clusters
3	Chao-Hsien Wu	Resource theory of non-steerability-breaking channel
4	Mao-Ting Wun	Analytically estimate quantum steering robustness of pure entangled state
5	Miu Ashiba	Systematic Analysis of Positron Binding to Halogenated Hydrocarbons
6	Tian-Shu Gou	Exceptional Topological Phase Transition in an Optical Mirror
7	Yuu Ishii	Theoretical clarification of H/D isotope effects on the phase transition temperature of K3H(SO4)2
8	Po-Yang Chen	Time-domain Measurement-based quantum computation on cloud quantum computer
9	Cheng-Yu Huang	Laser-Induced Photoresponse in MoS_2-Based Optoelectronic Devices
10	Taiga Ohnishi	Iterative synthesis of long-chain polyamines (LCPAs) with diverse chain lengths to elucidate their cell-penetrating activities
11	Shih-Chieh Chen	Development of a Portable Instrument for Laser-Assisted Microscopic Analysis of Materials
12	Haruki Nagata	Negative-Ion Mass Spectrometry of Ibuprofen and Its Analogues
13	Hsin-Sung Chen	Enhanced Stability of Gr_MoS2 and h-BN_MoS2 Heterostructures under Laser Illumination
14	Ibuki Ozawa	Synthetic studies of Scopadulciol, a novel anticancer drug lead compound
15	Juri Miyamoto	Optical properties of the extract of annealed C60 NWs
16	Kai-Wen Hsiao	Direct CVD growth of WxTi(1-x)S2 for Room-temperature layered ferromagnetic materials
17	Takumi Oriyama	Crystallization and evaluation of Thaumatin crystals with L-, D- tartrate
18	Lisa Ogata	Scanning Tunneling Luminescence measurements on C60 molecular films
19	Ming-Hsien Hsu	Surface characterization and control of skyrmions in van der Waals ferromagnet Fe3GaTe2
20	Momomi Morita	Measurements of coffee aromas using atmospheric pressure corona discharge ionization mass spectrometry
21	Min-Han Tsai	Logically Derived Sequence Tandem Mass Spectrometry for Structural Determination of Unusual Complex N-glycan in Eggs
22	Min-Jia Zhang	Inspection of Grain Boundary Structures of Large-Area Molybdenum Disulfide by Spectroscopic Mapping Technologies
23	Muhammad Yusuf Fakhri	Texture control to achieve high in-plane thermoelectric performance in polycrystalline tin monosulfide (SnS) co-doped with silver and sodium
24	Ping-Shen Chang	Study of Optical Chirality in Quasi-2D Chiral Perovskite Thin Films by Helicity-Resolved PL Spectroscopy
25	Ryota Araki	Theoretical Study of Passivation on Sn Perovskite Surface by Amine-based Molecules
26	Sumangaladevi Koodathil	Unveiling Local Activity in Layered TMDCs for Energy Conversion: A Combined SECM-AFM Approach
27	Wataru Nakajima	Preparation of SERS substrates by DC sputtering and annealing
28	Yu-Chieh Lo	Behavior of iron deposition on the surface structure and electrical properties of CrBr3 by scanning tunneling microscopy and spectroscopy
29	Wun-Long Li	Structural determination of fructooligosaccharides in onions using logically derived sequence tandem mass spectrometry
30	Yi-Chih Cheng	Gate-Driven Photoluminescence Modulation of Monolayer MoS2 FET

Stereoselectivity in Matching Partners: Navigating the Influence of Reaction Parameters in Glycosylation

Fizza Sabbor[1,2,3], Cheng-Chung Wang[1]

[1]Institute of Chemistry, Academia Sinica,
[2]Department of Chemistry, National Tsing Hua University, Hsinchu, Taiwan,
[3]Molecular Science and Technology (MST)- Taiwan International Graduate Program (TIGP)
sabbor0001@gate.sinica.edu.tw

ABSTRACT

The chemical synthesis of glycan chains relies heavily on glycosylation reactions capable of achieving efficient stereo- and regioselective glycosidic linkages. However, controlling stereoselectivity and achieving high yield in glycosylation is challenging due to the reaction's high degree of sensitivity, and the intricate mechanistic pathways influenced by various factors. In glycosylation, the optimized reaction parameters, and the process of partner matching involving relative reactivity values (RRV) of glycosyl donors, and acceptor nucleophilic constants (Aka) of acceptors, can be analogously likened to stereoselective glycosylation reactions. This study delves into the parallels between stereoselectivity and the dynamics of partner selection. We investigated the multifaceted interplay of factors such as temperature, solvent, concentration, stoichiometry, promoters, RRV of glycosyl donors, and Aka of acceptors, drawing analogies to the complexities of interpersonal relationships in glycosylation. Our investigation reveals that the low temperatures tend to promote β-glycosidic linkages, particularly with low RRV glycosyl donors. Conversely, higher temperatures favor α-glycosidic linkages, particularly with low Aka acceptors. Additionally, acetonitrile demonstrated a preference for β-selectivity while *p*-dioxane prefered α-selectivity, aligning with the solvent coordination hypothesis. Notably, employing a low Aka nucleophile consistently results in α-selectivity, regardless of diluted or concentrated reaction parameters. Glycosylations involving matching partners can be selectively tuned to the outcomes of either a 1:0.6 (α- β) ratio of one stereoisomer or a 1:3.7 ratio of the other by simply altering the stoichiometry of the reaction.

Mechanical properties of C_{60} nanowhiskers after heat treatment

Ayune Mizukami, Ryo Suzuki, Masaru Tachibana
Graduate school of Nanobioscience, Yokohama City University, Japan
e-mail: n245224a@yokohama-cu.ac.jp

ABSTRACT

C_{60} nanowhiskers (C_{60}NWs), solvated crystals, are one-dimensional fiber crystals grown by solution method. The solvated C_{60}NWs exhibited flexible behavior with large elastic deformation in air.[1,2] On the contrary, desolvated C_{60}NWs were very brittle after heat treatment at 250℃.[2] Recently, we found that higher-temperature treatment at 300℃ resulted in unique mechanical properties. In this presentation, we report the effect of higher-temperature treatment on the structure and mechanical properties of C_{60}NWs.

C_{60}NWs were grown by the liquid-liquid interfacial precipitation method with *m*-xylene and 2-propanol as good and poor solvent, respectively. The mechanical properties were measured by using bending test and nanoindentation test. The structure transformation due to the heat-treatment are examined by utilizing Field Emission-Scanning electron microscopy, Raman spectroscopy, Fourier transform infrared spectrometer and powder X-ray diffraction.

C_{60}NWs grown by *m*-xylene had fiber-like shapes and exhibited large elastic deformation in air as previous study.[1] C_{60}NWs after higher-temperature treatment at 300℃ exhibited larger elastic deformation and hardness than those at room temperature and after heat treatment at 250℃(fig.1). On the other hand, XRD showed that the crystal form of face-centered cubic(fcc) in the higher-temperature-treated samples was the same as that in the desolvated samples with brittleness heat-treated at 250℃(fig.2). Notably, Raman spectra showed that C_{60} cages can be disintegrated after the higher-temperature treatment at 300℃. These results indicate that the crystal form of fcc in desolvated C_{60}NWs is kept even after the higher-temperature treatment although C_{60} cages are disintegrated. These results means that the high-temperature treatment for C_{60}NWs can give rise to a new material with superior elastic properties and hardness, induced by the disintegration of C_{60} cages. The details will be discussed in light of structural transformation in the presentation.

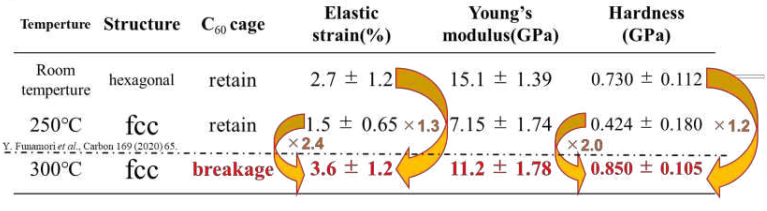

Fig.1 Comparison of structural states and mechanical properties of C_{60}-*m*-xylene at room temperature and after heating at various temperatures.

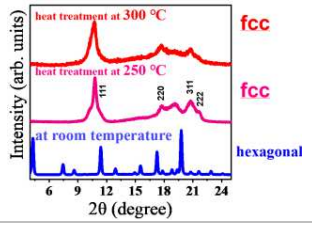

Fig.2 XRD pattern of C_{60}-*m*-xylene at various temperatures.

References

1. Y. Funamori *et al*., **Carbon**. 169, 65 (2020) 2. M. Watanabe *et al*., **J. Phys. Conf. Ser**. 159, 12009 (2009)

Will clathrin coated pits be always spherical?

Suguru Ushioda[1], Masashi Tachikawa[1]

1 Graduate school of Nanobioscience, Yokohama city university, Kanagawa, Japan
E-mail: n245204b@yokohama-cu.ac.jp

Abstract

We developed a new model for the shapes of domains in clathrin-mediated endocytosis. The shapes of clathrin-coated pits (CCPs) change with varying membrane tension[1, 2]. We discussed the diversity of domain shapes and constructed a physical model assuming the domain can be spherical, partially spherical, elongated, or split. As a result, we found regions of solutions where elongation and splitting are energetically stable.

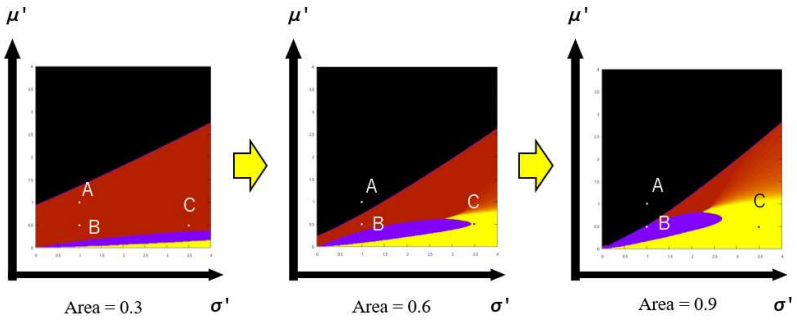

Fig.1 Relationship between the changes of membrane area and of domain shape
Three dots in each figure represent (σ', μ') = A(1, 1), B(1, 0.5), and C(3.5, 0.5). The black, red, yellow, and purple regions indicate a sphere, partial sphere, elongation, and split, respectively. "Area" refers to the surface area of the domain.

References

1. Pierre Sens & Matthew S. Turner, "Budded membrane microdomains as tension regulators", *Physical Review E* **73**, 1-4 (2006).
2. Mohammed Saleem, Sandrine Morlot, Annika Hohendahl, John Manzi, Martin Lenz & Aurélien Roux, "A balance between membrane elasticity and polymerization energy sets the shape of spherical clathrin coats", *Nature Communications* **6**, 1-10 (2015).

Characteristics in 1D & 2D chiral perovskite single crystals and thin films

Chia-Hsiang, Chuang

NTNU
e-mail: vernier0914@gmail.com

ABSTRACT

It is easy to say that my research is to compare with 1D & 2D perovskites different. In the begging, I'll show difference between 1D & 2D perovskite such as CD spectrum, PL ,and LED. In my research circular dichroism (CD) spectrum is the most important part because most of teams trying to grow up the g-abs (so call the g value). So that we compare 1D & 2D perovskite to improve the low dimension is greater than high dimension.

Although it can identify which optical characteristics is greater than other, we still cannot identify the electric signal is better. That is why I make it to LED to make sure that if there are different. We can know that if one makes perovskite film too heavy than one can get more strong CD signal, but the film too heavy one cannot have electric signal. In order to get external quantum efficiency (EQE) one show let the film more thinner, so this is what I want to do next. To find the adjustment film to have CD signal and also have better EQE.

References

1. Yangyang Dang , Xiaolong Liu, *J. Phys. Chem. Lett.* 2020, 11, 5, 1689−1696(February 10, 2020)
2. Ying Lu, Qian Wang,Advance functional material **Volume31, Issue43**(06 August 2020)

Atomic excitation trapping in dissimilar atomic array with chiral coupling

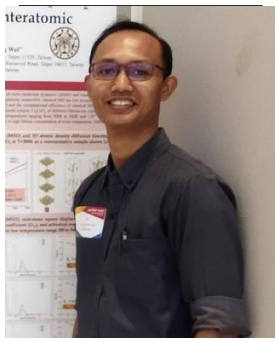

I Gusti Ngurah Yudi Handayana[1,2,3,*], Chun-Chi Wu[3], Sumit Goswami[3], Ying-Cheng Chen[3], and H. H. Jen[3,1,4,†]

[1]Molecular Science and Technology Program, Taiwan International Graduate Program, Academia Sinica
[2]Department of Physics, National Central University
[3]Institute of Atomic and Molecular Sciences, Academia Sinica
[4]Physics Division, National Center for Theoretical Sciences
e-mail: [*]ngurahyudi@unram.ac.id
[†]sappyjen@gmail.com

ABSTRACT

An atomic array coupled to a one-dimensional nanophotonic waveguide allows photon-mediated dipole-dipole interactions and nonreciprocal decay channels[1–4]. Such an array possesses many intriguing quantum phenomena due to its distinctive and emergent quantum correlations[5–7]. In this atom-waveguide quantum system, we theoretically investigate the atomic excitation dynamics and its transport property, specifically at an interface of dissimilar atomic arrays with different interparticle distances. We find that the atomic excitation dynamics is highly dependent on the interparticle distances of dissimilar arrays and the directionality of nonreciprocal couplings. By tuning these parameters, a dominant excitation reflection can be achieved at the interface of the arrays in the single excitation case. We further study two effects on the transport property of external drive and of single excitation delocalization over multiple atoms where we manifest a rich interplay between multisite excitation and the relative phase in determining the transport properties. Finally, we present an intriguing trapping effect of atomic excitation by designing multiple zones of dissimilar arrays. Our results can provide insights into nonequilibrium quantum dynamics in dissimilar arrays, and they can shed light on confining and controlling quantum registers useful for quantum information processing.

References

1. Y. G. Huang, G. Chen, C. J. Jin, W. M. Liu, & X. H. Wang, **Physical Review A,** *85*, 053827 (2012).
2. H. Pichler , T. Ramos, A. J. Daley, & P. Zoller, **Physical Review A,** *91*, 042116 (2015).
3. P. Lodahl, *et al.,* **Nature,** *541*, 473–480 (2017).
4. A. S. Sheremet, M. I. Petrov, I. V. Iorsh, A. V. Poshakinskiy, & A. N. Poddubny, **Reviews of Modern Physics,** *95*, 015002 (2023).

5. H. H. Jen, **Physical Review A,** *102*, 043525 (2020).
6. C. C. Wu, *et al.,* **Physical Review Research,** *6,* 013159 (2024).
7. S.-H. Chung, *et al.,* **Physical Review Research,** *6,* 023232 (2024).

Hydrogenation Effect on Antisymmetric Magnetoresistance in Co/Pd Multilayers

Yan-Ru Chu[a], Chun-Tse Hsieh[a], Chak-Ming Liu[a], Jhen-Yong Hong[b], Wen-Chin Lin[a]

[a] Department of Physics, National Taiwan Normal University, Taipei, Taiwan
[b] Department of Physics, Tamkang University, New Taipei City, Taiwan
yrchu1207@gmail.com

ABSTRACT

In Co/Pd multilayers, we observe controllable anomalous magnetoresistance (MR) influenced by the unique geometric relationship among current, magnetization, domain wall motion, and hydrogen loading. An antisymmetric MR is measured in the ambient condition, because of the presence of perpendicular magnetic anisotropy (PMA) and the asymmetric domain wall motion, as shown in Fig. 1(a)-(e). The investigation, including magnetic domain images acquired through the Magneto-Optical Kerr Microscope and transport properties measurements, attributes the antisymmetric MR to the anomalous Hall effect within the PMA sample. Upon hydrogen absorption, the magnetization becomes tilted and then turns to in-plane anisotropy. Meanwhile, the MR curve sensitively changes with slight hydrogenation, corresponding to the spin-reorientation transition process in the Co/Pd multilayer, as shown in Fig. 1(f)-(h). Upon more hydrogen exposure, an obvious MR is only present when an in-plane magnetic field is applied, signifying a transition to in-plane anisotropy. This study emphasizes the tunable nature of MR in the Co/Pd multilayer system, providing novel insights into the diversity of MR, which holds the potential to influence the multifunctionality of spintronic devices. The high sensitivity of PMA and MR behavior to a few mbar hydrogen pressures suggests its potential for application.

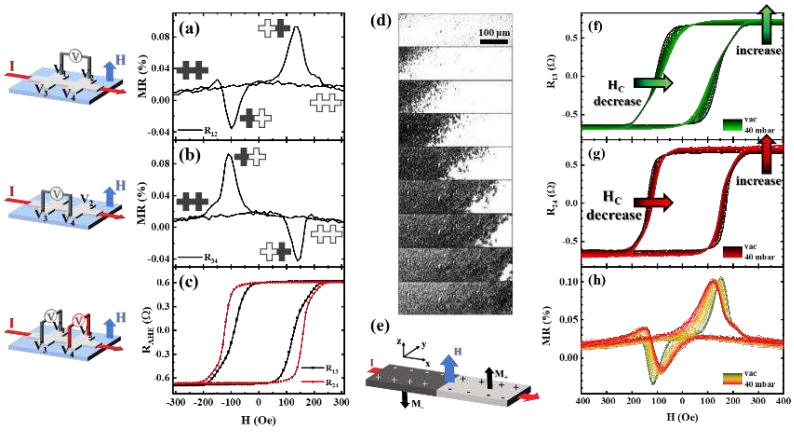

References

1. P.-C. Chang, et al., **Hydrogen-mediated magnetic domain formation and domain wall motion in Co30Pd70 alloy films**, *Sci. Rep. 8*, 6656 (2018).
2. X.-M. Cheng, et al., **Antisymmetric Magnetoresistance in Magnetic Multilayers with Perpendicular Anisotropy**, *Phys. Rev. Lett. 94*, 017203 (2005).

Uniform Growth and Characterization of Hexagonal Boron Nitride (h-BN) on Dielectric Substrates for Quantum Technology Applications

Suraj Singh[1,2], Mario Hofmann[3], Ya-Ping Hsieh[1,2]
Affiliation: [1]Institute of Atomic and Molecular Sciences, Academia Sinica, Taiwan,
[2]International Graduate Program of Molecular Science and Technology, National Taiwan University, Taiwan
[3] Department of Physics, National Taiwan University, Taipei 10617, Taiwan
e-mail: singh.suraj.ntu@gmail.com

ABSTRACT

Quantum emitters are pivotal in advancing quantum technology applications such as Quantum Information Processing, Long Inter-planetary Communication, and Secure Cyber Security Networks. At the core of these advancements are Quantum Bits, the fundamental units of quantum computers. Hexagonal Boron Nitride (h-BN), a 2D material, offers significant advantages for hosting diverse quantum emitters, including single-photon emitters and vacancy centers, due to its excellent photostability, brightness, and sharp emission lines[1].

Unlike diamond and SiC, h-BN can be precisely synthesized via Chemical Vapor Deposition (CVD), facilitating scalability and integration with other materials. Its wide bandgap (~6 eV) ensures efficient room-temperature operation, making it highly practical for quantum applications. Additionally, h-BN's unique properties, such as high thermal conductivity, mechanical strength, and chemical stability, along with the ability to introduce and control various defects, make it a versatile platform for tuneable and efficient quantum emitters.

In this study, our focus on the continuous growth of h-BN on dielectric substrates. We synthesize h-BN thin films on Si/SiO_2 substrates using low-pressure CVD, aiming to produce higher quality films compared to previous reports [2,3]. Moreover, various characterization techniques, including Raman spectroscopy, atomic force microscopy, and photoluminescence, employed to analyse the quality and properties of the synthesized h-BN films. This comprehensive characterization will provide insights into the structural and optical properties of h-BN, setting the stage for further advancements in quantum technologies.

References

1 N. Mendelson, *et al.* Identifying carbon as the source of visible single-photon emission from hexagonal boron nitride. *Nature materials* **20**, 321-328 (2021).

2 D. Liu, *et al.* Conformal hexagonal-boron nitride dielectric interface for tungsten diselenide devices with improved mobility and thermal dissipation. *Nature communications* **10**, 1188 (2019).

3 M. Yamamoto, *et al.* Low-temperature direct synthesis of multilayered h-BN without catalysts by inductively coupled plasma-enhanced chemical vapor deposition. *ACS omega* **8**, 5497-5505 (2023).

Probing Phonon Symmetry Breaking in MoS_2 Using Polarized Raman Spectroscopy

Shih-Po Chien, Ting-Hua Lu, Yann-Wen Lan

Affiliation: Department of Physics, National Taiwan Normal University, Taipei 116, Taiwan
e-mail: ywlan@ntnu.edu.tw

ABSTRACT

Polarized Raman spectroscopy is widely used to determine the symmetry of materials and their vibrational modes. Elliptically polarized light as the excitation source has been reported to induce symmetry breaking in the doubly degenerated E_{2g} vibrational mode in highly symmetric D_{3h} point group materials, such as MoS_2 and hBN, due to the nontrivial symmetric properties and non-integer spin angular momentum (SAM) coupling with in-plane phonon fields. In this work, we applied various configurations of polarized Raman spectroscopy to study the in-plane phonons in MoS_2, analyzed using Jones calculus. We reproduced the symmetry breaking in the E_{2g} signal through polarization-resolved Raman spectroscopy and ruled out the simplest combination of vibrational modes using angle-resolved Raman spectroscopy. Helicity-resolved Raman spectroscopy revealed that the doubly degenerated E_{2g} modes at the Γ point are incoherent due to variations in electronic transition paths. Meanwhile, it has been theoretically predicted that the pseudoangular momentum (PAM) of phonons at the K point can be directly detected via electron energy loss spectroscopy (EELS), highlighting interactions between PAM of phonons and the excitation. Future research should focus on applying light with SAM or OAM to detect phonon modes with PAM. Additionally, exploring double resonance could provide further insights into phonon modes away from the Γ point, such as at the K or K' points. This study provides a methodology to reveal detailed information even in highly symmetric materials, demonstrating the potential to introduce an extra degree of freedom of information that can be utilized in phononics studies.

References

1. T.-D. Huang, K. B. Simbulan, Y.-F. Chiang, Y.-W. Lan, and T.-H. Lu, **Symmetry breaking of in-plane Raman scattering by elliptically polarized light in MoS_2**, *Phys. Rev. B*, 100, 195414 (2019).
2. S.-P. Chien, Y.-C. Chang, K. B. Simbulan, S. Saha, Y.-F. Chiang, R. K. Saroj, G.-C. Yi, S. Arafin, T.-H. Lu, Y.-W. Lan, **Helicity exchange and symmetry breaking of in-plane phonon scattering of h-BN probed by polarized Raman spectroscopy**, *Appl. Phys. Lett.*, 121, 182203 (2022)
3. M. R. Bourgeois, A. W. Rossi, and D. J. Masiello, **Strategy for Direct Detection of Chiral Phonons with Phase-Structured Free Electrons**, *ArXiv*, 2405.01826 (2024)
4. R. N. Gontijo, G. C. Resende, C. Fantini, and B. R. Carvalho, **Double resonance Raman scattering process in 2D materials**, *Journal of Materials Research*, 34, 1976–1992 (2019)

Theoretical analysis of positronic compounds of fluorine molecular dianions using quantum Monte Carlo method

Kentaro Numata[1], Daisuke Yoshida[2], Masanori Tachikawa[1], Yukiumi Kita[1]

affiliation: [1] *Graduate School of Nanobioscience, Yokohama City University, Japan*

[2] *Graduate School of Science and Faculty of Science. Tohoku University, Japan*

e-mail: n235221a@yokohama-cu.ac.jp

ABSTRACT

Positrons are the antiparticles of electrons; they have the same mass and spin as electrons, but a positive charge. Recently, Reyes *et al.* predicted the existence of the complex $[X^-; e^+; X^-]$ $(X = H, Li, F)$ of a diatomic molecular dianion and a positron theoretically [1,2]. They showed that diatomic molecular dianions, which are generally unstable and cannot exist, can exist stably through covalent bonding via positrons (positron bonding). However, their predictions are based on a small-scale configuration interaction method with insufficient computational accuracy, and their results are not sufficiently reliable. In this study, thus, we theoretically analyzed the stabilization mechanism of the positron complex of the fluorine molecular dianion $[F^-; e^+; F^-]$ using the quantum Monte Carlo (QMC) method, one of the most accurate first-principles methods.

In QMC calculations, we performed (i) variational Monte Carlo (VMC) calculations with the Slater-Jastrow type function and (ii) diffusion Monte Carlo (DMC) calculations, which give the numerical exact ground state by an imaginary-time evolution.

Figure 1 shows the total energy profiles of $[F^-; e^+; F^-]$ as a function of the inter-nuclear distance (R) with each method. The $[F^-; e^+; F^-]$ system has a single minimum in the range of 1 to 6 Å for all methods, and the equilibrium internuclear distance was found to be shortened by incorporating many-body effects. Since the total energy with our DMC calculation is lower than the energy thresholds of other possible dissociation channels, we conclude that the $[F^-; e^+; F^-]$ system can exist theoretically within a specific lifetime. Other details will be presented on the day.

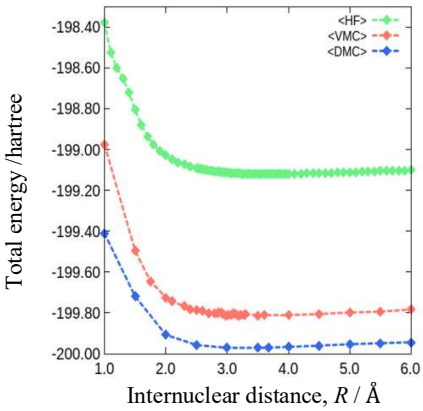

Figure 1: Total energy of $[F^-; e^+; F^-]$

References

1. J. Charry, et al., *Angew. Chem. Int. Ed.*, **57**, 29 (2018).
2. A. Reyes, et al., *Chem. Sci.,* **11**, 44 (2020).
3. M. Tachikawa, *Chem. Phys. Lett.* **350**, 269 (2001).
4. Y. Kita, et al., *Chem.Phys.* **135,** 054108 (2011).

Correlated photoluminescence blinking phenomenon on InGaN/GaN NanoPillars structures

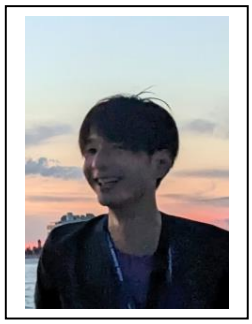

Kotaro Oikawa and Ruggero Micheletto
Yokohama City University, Department of Materials System Science
e-mail: n235301d@yokohama-cu.ac.jp and ruggero@yokohama-cu.ac.jp

ABSTRACT

Light-emitting devices that take advantage of the wide bandgap characteristics of InGaN/GaN are widely used in the industry. However, inhomogeneities have been reported in their photoluminescence (PL) mapping at the nanometer and submicrometer scale even in samples of high crystal quality. In addition, a blinking phenomenon (time variation of PL intensity) under photoexcitation has been reported in relation to these inhomogeneities[1]. The reason why this blinking phenomenon occur is still unclear, it has been observed in quantum dots and other single and multilayer quantum wells structures. Nevertheless, there are very few publications on nanopillar InGaN quantum well samples, which are the focus of this research. Here, we report and analyzed the behavior of the blinking phenomena on a nanopillars sample for the first time. We noticed that the blinking of the pillars is somehow synchronized on a long time scale among several spatially separated nanopillars. We demonstrated that the synchronization is not due to random intensity fluctuations. We suggest instead that the synchronization is caused by a non-linear response of the quantum wells to the UV source. In other words, when the stimulation intensity surpass a certain value, it triggers a ON/OFF state switch in the photoluminescence of some of the pillars. Even if preliminary, our study helps to provide clues to understanding the mechanism of the occurrence of the blink phenomenon.

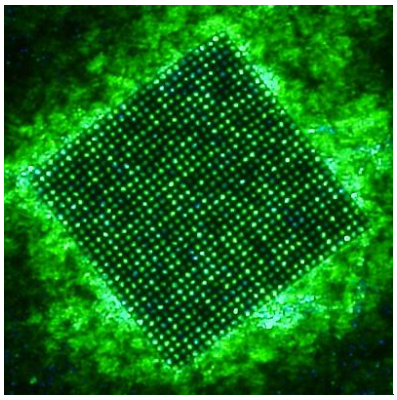

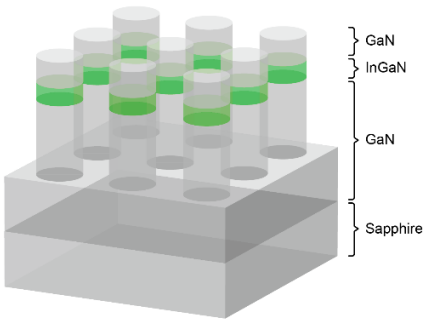

References

1. (times new roman 12pt) R. Micheletto *et al.*, **Applied Physics Letters**, *88*, Page-061118 (2006).

Absolute Line Strength and Rovibrational Spectrum of Hydroperoxyl Radical in the ν_3 Fundamental Band

Che-Wei Chang[1,2], I-Yun Chen[1,3], Pei-Ling Luo[1]

[1]Institute of Atomic and Molecular Sciences, Academia Sinica, Taipei, Taiwan

[2]Molecular Science and Technology, Taiwan International Graduate Program

[3]Department of Chemistry, National Taiwan University, Taipei, Taiwan

e-mail: victorchang12323@gmail.com

ABSTRACT

Hydroperoxyl radical (HO_2) is an important species in atmospheric science. In this work, we carried out flash photolysis with the flowing mixture of O_2, CH_3OH, and Cl_2, which generated Cl atom. Subsequently, Cl atom reacted with CH_3OH to produce HCl and CH_2OH. CH_2OH reacted with excessive amount of O_2 to produce HO_2 and HCHO. The absolute line strength of HO_2 ν_3 transition is accurately determined with an uncertainty down to 4% through simultaneous measurement of HO_2 and HCl time-resolved absorption spectra in the 9 μm and 3 μm spectral region, respectively, with a time resolution of tens of μs by using synchronized two-color time-resolved dual-comb spectroscopy. Furthermore, the high-resolution broadband spectrum of the relative line intensity of HO_2 OO stretching was measured over more than 30 cm^{-1} to give the band strength in the ν_3 fundamental band.

Morphology control of protein crystals by hydrogel

Miina Suzuki, Ryo Suzuki, Masaru Tachibana
Graduate school of Nanobioscience, Yokohama City University, Japan
e-mail: n245213d@yokohama-cu.ac.jp

ABSTRACT

High-quality protein crystals are important for understanding the three-dimensional(3D) structure and properties of protein via X-ray diffraction. To produce high-quality protein crystals, crystal growth under various external conditions has been conducted. In this study, we focus on the gel method which is one of the crystallization methods under different growth environment. The protein crystals grown in hydrogel possess interesting properties, such as growth incorporating gel, reduction of radiation damage by X-ray [1] and drastic improvement in fracture strength [2]. However, the detailed effects for the crystal growth of protein crystals in hydrogels remain unclear. The findings are expected to be applicable to drug discovery research and gel-protein composite materials.

In this study, tetragonal hen egg-white lysozyme (T-HEWL) crystals were grown at various hydrogel concentrations. The growth of protein crystals in the gel can be achieved by mixing the protein solution with the gel. Fig.1a shows the typical shape of T-HEWL crystal. Fig. 1(b)-(e) show optical microscope images of the obtained crystals at each gel concentrations between 1.0 and 5.0 wt.%, respectively. It was clearly observed that the aspect ratio of <001> and <110> direction was changed with gel concentrations of 1.5 wt.% and below. Remarkably, at gel concentrations of 2.0 wt.% and above, we found obvious changes of crystal morphology. The concavity appeared at the centers of the crystal faces {011} and {101} (Fig.1c). At the gel concentration of 3.0 wt.%, the edges of the crystals became rounded, and the boundaries between faces disappeared (Fig.1d). Furthermore, the crystals formed spherical shapes (Fig.1e), with the proportion of spherical crystals increased with higher gel concentrations. This behavior is attributed to the diffusion lag of protein molecules and the reduction of surface free energy in hydrogel media. In the presentation, the details of the crystal morphology changes at each gel concentrations and factors contributing to morphological changes is discussed.

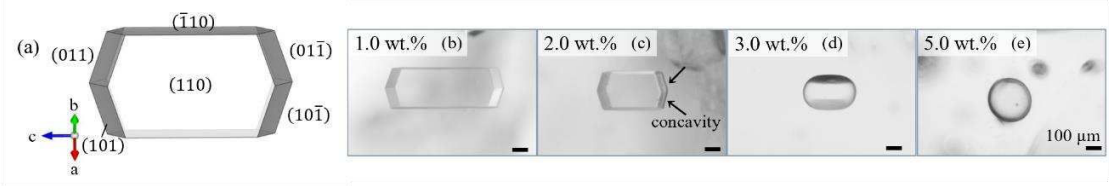

Figure 1. (a) schematic diagram of the tetragonal lysozyme crystal. (b)-(e) an optical microscope image of the obtained crystals at each gel concentrations.

References

1) S. Sugiyama *et al*., **J. Am. Chem. Soc.** *134*, 5786-5789 (2012).
2) R. Suzuki *et al*., **ACS Appl. Bio Mater.** *6*, 965-972 (2023).

Computational study on the role of residues near the chromophore in Enhanced Green Fluorescent Protein

Mio Takakuwa, Yukiumi Kita, Tomomi Shimazaki, Masanori Tachikawa

Department of Materials System Science,
Graduate School of NanoBioScience, Yokohama City University
n245303c@yokohama-cu.ac.jp

ABSTRACT

Green Fluorescent Proteins (GFPs) emit a green glow, and their variant, Enhanced GFP (EGFP), shines even brighter, making it extensively used in bio-imaging applications[1]. Both GFP and EGFP have their chromophore (CRO) centrally located, which is crucial for luminescence. These proteins autonomously synthesize their CROs, which emit light upon excitation. In EGFP, residues surrounding the CRO, such as Arg96 and Thr203, have been experimentally shown to play significant roles, as depicted in Figure 1. However, the theoretical details of their individual impacts remain poorly understood. Thus, this study theoretically investigates the influence of these residues on the CRO, their hydrogen-bonded structures, and fluorescence spectra, aiming to clarify the roles of Arg96 and Thr203.

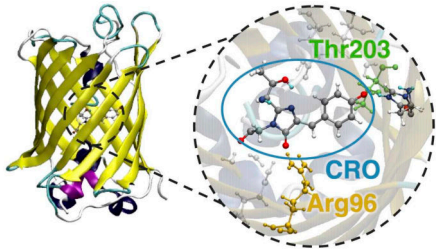

Figure 1. The location of CRO, Arg96 and Thr203 in EGFP.

From the structure of EGFP (PDB ID: 6L26), we created the "EGFP model" (207 atoms) incorporating residues directly hydrogen-bonded to the CRO, the "model without Arg96" (181 atoms) and the "model without Thr203" (191 atoms) excluding only Arg96 or Thr203, respectively. We performed the geometry optimization calculations with the multi-component theory extended to density functional theory[2].

Figure 2 shows that the absorption spectra of each model. In the model without Arg96 and Thr203, the absorption peak is blue-shifted; namely, with the presence of Arg96 and Thr203, the peaks are red-shifted. Furthermore, it has been demonstrated that these residues significantly affect the protonated states and charge distribution of CRO. More complete results have been reported in our recent paper[3].

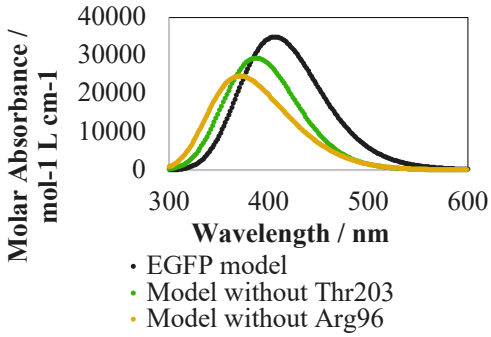

Figure 2. Absorption spectra of each model.

References

1. R. Y. Tsien, **Annu Rev Biochem.**, *67*, 509- (1998).
2. T. Udagawa, *et al.* **J. Chem. Phys**., 125, 244105 (2006).
3. M.Takakuwa, *et al*. **Bull. Chem. Soc. Jpn**., *96*, 711- (2023).

Exploring the influence of S/Cl sites' mixing on the lithium diffusion behaviors of $Li_{x+6}PS_5Cl$

Lily M Angraini[1,2,3], Cheng-Rong Hsing[4], Ching-Ming Wei[3,5]

[1]International Graduate Program of Molecular Science Technology (NTU-MST), National Taiwan University, No. 1, Sec. 4, Roosevelt Road, Taipei 10617, Taiwan
[2]Taiwan International Graduate Program (TIGP), Academia Sinica No. 128, Sec. 2 Academia Road, Taipei 11529, Taiwan
[3]Institute of Atomic and Molecular Sciences, Academia Sinica, Taipei 10617, Taiwan
[4]Division of Natural Science, Center for General Education, Chang Gung University, Taoyuan City, 33302, Taiwan
[5]Institute of Physics, Academia Sinica, Nankang 11529, Taiwan

cmw@phys.sinica.edu.tw

ABSTRACT

Due to its exceptionally high ionic diffusion coefficient and stability, the compound $Li_{6+x}PS_5Cl$, lithium argyrodite, has demonstrated significant potential as an electrolyte in solid-state batteries. Structural disorder and mixing of S/Cl sites found by experimental XRD are expected to affect how Li ions move through this material significantly; however, how this affects lithium diffusion and its correlation with the diffusion coefficients still need to be determined and answered. In this work, we perform large-scale molecular dynamics simulations on $Li_{6+x}PS_5Cl$ based on machine-learning interatomic potentials fitted from ab initio molecular dynamics simulations. We carefully studied the influence of S/Cl site mixing on the lithium diffusion behaviors in $Li_{6+x}PS_5Cl$. The results indicate that increased or decreased lithium concentration away from $Li_{6+x}PS_5Cl$, or S/Cl sites' mixing, can increase the diffusion coefficient by two-order magnitude from $10^{-7}cm^2/s$ to 10^{-5} cm^2/s. The Arrhenius equation can describe lithium atoms' diffusion behavior well, where the activation barrier ranges from 108 to 187 meV. The small diffusion barriers provide the fundamental origin for the fast diffusion behaviors of lithium atoms.

References

1. Z. Dheng, Z. Zhu, I.H.Chu, S.P.Ong, **Chem. Matter**, Data-Driven First-Principles Methods for the Study and Design of Alkali Superionic Conductors, 29, 281-288. (2017).
2. A. Baktash, J.C.Reid, T.Roman, D.J.Searles, **Nature Computational Material,** Diffusion of lithium ions in Lithium-argyrodite solid-state electrolytes, 162, (2020)
3. R. Schelenker, A.Hansen, et al. **Chem. Matter.** Structure and diffusion pathways in Li6PS5Cl argyrodite from neutron diffraction, pair-distribution function analysis, and NMR, 32, 8420–8430, (2020).
4. Novikov, I. S., Gubaev, K., Podryabinkin, E. V & Shapeev, A. V. *Mach Learn Sci Technol* **2**, 025002 (2021).
5. Podryabinkin, E. V. & Shapeev, A. V. *Comput Mater Sci* **140**, 171–180 (2017).

Optoelectronic Properties of Chiral NEA Quasi-2D Perovskite Films with Different Precursor Ratios

Pei-Hsuan Lo, Yu-Chiang Chao
Department of Physics, National Taiwan Normal University
e-mail: hsuan55864@gmail.com, ycchao@ntnu.edu.tw

ABSTRACT

Under the addition of large cations, 3D perovskite CsPbBr3 transforms into quasi-2D perovskite. In this research, chiral cation 1-(1-naphthyl)ethylamine (NEA) in different proportions is introduced to CsPbBr3, resulting in a chiral quasi-2D perovskite. Circular dichroism (CD) and absorption spectra showed an intensity increase, along with a blue shift in the absorption peak, confirming the transformation induced by chiral NEA. This transformation was further confirmed by PL spectra. SEM images showed an increase in surface roughness when adding chiral NEA at a ratio of 2.5. To achieve the goal of making spin LEDs, following research focused on a precursor ratio of 2:1:1 with the highest concentration of chiral NEA. Magnetic Circular Dichroism (MCD) measurements of the 2:1:1 ratio perovskite thin film showed Cotton effects and Zeeman splitting, corresponding to excitonic features of the absorption spectra. The "g value" calculated by excluding the effect of film thickness on CD intensity falls within the range of $\pm 3 \times 10^{-3}$ after applying a magnetic field. Finally, chiral perovskites were applied in spin LEDs with chiral-induced spin selectivity. Despite a decrease in current density after adding chiral layers, EQE and Luminous current efficiency showed no significant changes. This indicates that the addition of chiral layers did not improve the device performance, suggesting further electrical characterization for future improvement.

References

1. D Di Nuzzo, L Cui, JL Greenfield, B Zhao, RH Friend, SCJ Meskers. **ACS nano,** *14.6,* 7610-7616 (2020).
2. LS Yang, EC Lin, YH Hua, CA Hsu, HZ Chiu, PH Lo, Yu-Chiang Chao. **ACS Applied Materials & Interfaces,** *14.48,* 54090-54100 (2022).

A magnetic micro-actuator based on particle jamming

Khalil ur Rehman[1,2,3,4], Ya-Ping Hsieh[1,3*] and Mario Hofmann[4*]

[1]MST, TIGP, Academia Sinica; Taipei, Taiwan (R.O.C).
[2]International Graduate Program of Molecular Science and Technology, National Taiwan University; Taipei, Taiwan (R.O.C).
[3] IAMS, Academia Sinica; Taipei, 106, Taiwan (R.O.C).
[4]Department of Physics, National Taiwan University; Taipei, 106, Taiwan (R.O.C).
*mario@phys.ntu.edu.tw
*yphsieh@gate.sinica.edu.tw

ABSTRACT

Magnetic microactuators and microrobots have the potential to revolutionize remote manipulation and swarm-based collaboration. Unfortunately, conventional approaches to controlling individual magnetic systems cannot be shrunk to the microscale due to fundamental challenges in the generation and modification of magnetic fields. We here demonstrate a novel actuation mechanism that imparts magnetic microactuators with unprecedented ease of fabrication and dimensional scaling. Through mechanical jamming in binary particle mixtures, magnetic ordering and pronounced anisotropy could be induced. Combined simulation and experimental investigation confirm the importance of arresting forces from neighboring particles as the origin of this behavior. This sensitivity of magnetic properties on assembly morphology can be exploited to produce novel actuators that utilize minute changes in particle size or pressure. We demonstrate the transduction of particle swelling into magnetic torque locking that enables active magnetic control in microrobots for future remote operating applications.

Utilizing Light's Orbital Angular Momentum to Boost Photocurrent in MoS_2 Transistors

Ye-Ru Chen[1], Kristan Bryan Simbulan[2], Guan-Hao Peng[3], Yu-Chen Chang[1], I-Tong Chen[1], Han-Chieh Lo[1] Shao-Yu Chen[4], Shun-Jen Cheng[3], Ting-Hua Lu[1*], Yann-Wen Lan[1*]

[1]Deparment of Physics, National Taiwan Normal University, Taipei, Taiwan

[2]Department of Mathematics and Physics, University of Santo Tomas, Manila, Philippines

[3] Department of Electrophysics, National Yang Ming Chiao Tung University, Hsinchu, Taiwan

[4] Center of Atomic Initiative for New Materials, National Taiwan University, Taipei, Taiwan

*Email of the Corresponding author: ywlan@ntnu.edu.tw

ABSTRACT

The use of orbital angular momentum (OAM) in light introduces new possibilities for transitions that were previously restricted due to momentum conservation laws. When this light interacts with Transition Metal Dichalcogenides (TMDs), it enables targeted excitonic transitions. This study focuses on the optical and electrical behavior of a molybdenum disulfide (MoS_2) field-effect transistor (FET), utilizing OAM light for excitation. Our observations reveal a decrease in exciton photoluminescence (PL) and an increase in photoconductance as the OAM intensity increases. This indicates an inverse relationship between exciton-bound states and free carriers. We suggest that the extra momentum from OAM light reduces optical emission and aids in exciton dissociation, thereby boosting photoconductance. Our findings offer insights into using OAM light to enhance photocurrent on MoS_2-based FETs.

Exploring Exciton-Phonon Interactions in Photoexcited MoS_2 by Polarized Raman Spectroscopy

Yu-Chen Chang[1], Yu-Chiao Chan[1], Yann-Wen Lan[1], and Ting-Hua Lu[1*]

[1]Department of Physics, National Taiwan Normal University, Taipei, Taiwan

e-mail: 81041002s@gapps.ntnu.edu.tw

ABSTRACT

Double resonance Raman scattering occurs when the excitation energy closely aligns with the bandgap of a transition metal dichalcogenide (TMD), resulting in additional peaks in the Raman spectrum. The exciton-phonon interactions in these intervalley scattering processes are predominantly shaped by the interplay between deformation potential (DP) and Fröhlich interaction (FI), which influences the polarization characteristics of the scattered light[1,2]. To better understand the physical properties of novel two-dimensional (2D) materials, in this study, we employed a polarized Raman spectroscopy to investigate the polarization characteristics of the second-order Raman peak resulting from resonance excitation. The linearly and circularly polarized excitation light are utilized into polarized Raman spectroscopy to investigate the polarized phonon in MoS_2 under double resonance Raman scattering. As the temperature decreases from 300K to 77K, the dominance of FI strengths with a restricted energy-level distribution of electron transitions leads to a reversal in the polarization of the b-mode Raman scattering. The phenomenon elucidates the distinct interaction strengths among excitons and phonons in MoS_2, which can be effectively analyzed through polarized Raman spectroscopy. These results provide an important technique for exploring light-matter interactions in novel 2D materials, thereby advancing the development of optoelectronic applications.

References

1. Y. Zhao, S. Zhang, Y. Shi, Y. Zhang, R. Saito, J. Zhang, L. Tong, **ACS nano**, *14.8*, 10527-10535- (2020).
2. B. R. Carvalho, Y. Wang, S. Mignuzzi, D. Roy, M. Terrones , C. Fantini, ... & M. A. Pimenta, **Nature communications**, *8(1)*, 1-8- (2017)

Fast generation of multipartite entanglement in non-Hermitian qubits

C. G. Feyisa[1,2,4,*] J. S. You[5], H. Y. Ku[5,†] and H. H. Jen [1,2,3‡]

[1]Institute of Atomic and Molecular Sciences, Academia Sinica, Taipei 10617, Taiwan [2]Molecular Science and Technology Program, Taiwan International Graduate Program, Academia Sinica, Taiwan
[3]Physics Division, National Center for Theoretical Sciences, Taipei 10617, Taiwan
[4]Department of Physics, National Central University, Taoyuan 320317, Taiwan and
[5]Department of Physics, National Taiwan Normal University, Taipei 11677, Taiwan
∗ chimdessagashu@gmail.com
† huan.yu@gapps.ntnu.edu.tw
‡ sappyjen@gmail.com

ABSTRACT

Open quantum systems are susceptible to losing information, energy, and particles to their surrounding environment. One effective strategy to mitigate these losses is to transform them into advantages through tailored non-Hermitian quantum systems. In this work, we theoretically investigate fast generation of multipartite entanglement in superconducting non-Hermitian qubits. Our findings reveal that weakly coupled non-Hermitian qubits can accelerate entanglement generation by thousands of times compared to Hermitian qubits, especially when approaching the 2^n-th order exceptional points of n qubits from the PT-symmetric regime. Furthermore, we generate multipartite GHZ states in the Hermitian limit with a high fidelity of around 0.999 by strongly driving the qubits in the weak coupling regime. Our approach is scalable to a large number of qubits, presenting a promising pathway for advancing quantum technologies through the exploration of non-Hermiticity and higher-order exceptional points in many-body quantum systems.

References

1. M. Naghiloo, M. Abbasi, Y. N. Joglekar, and K. Murch, **Nat. Phys.**,*15*, 1232- (2019).
2. W. Chen, M. Abbasi, Y. N. Joglekar, and K. W. Murch, **Phys. Rev. Lett.**, *127*, 140504- (2021).
3. Z.-Z. Li, W. Chen, M. Abbasi, K. W. Murch, and K. B. Whaley, **Phys. Rev. Lett.**, *131*, 100202- (2023)

Theoretical study on dissociation reaction of nitrogen molecules on lithium clusters

Go Fujihara, Makito Takagi, Tomomi Shimazaki.
Materials System Science Major, Graduate School of Nanobioscience,
Yokohama City University
e-mail: n245223g@yokohama-cu.ac.jp

ABSTRACT

【Background】

Currently, ammonia is widely used in the chemical industry for fertilizers and chemicals. Ammonia is mainly synthesized by the Haber-Bosch method, which consumes a huge amount of energy due to the high temperature and high pressure conditions are required, and emits a large amount of carbon dioxide. Thus, a clean ammonia synthesis method is required. Recently, a new method for the synthesis of ammonia by lithium-mediated electrochemical nitrogen reduction has been reported as one of the cleanest ammonia synthesis methods.[1] This method has advantages such as small-scale synthesis at room temperature and pressure and nearly 100% Faraday efficiency. However, detailed reaction mechanisms are still unknown, and it has not yet been implemented in practical applications.[2]

In this study, to elucidate mechanism, we performed DFT calculation and analyzed the dissociation reaction of nitrogen molecules (N_2) on Li clusters, which is considered the first step of the reaction. We also analyzed the effects of the number of hydrogen atoms added to the nitrogen, the overall charge of the system, and the cluster size.

【Computational Methods】

All electronic structure calculation were performed at the B3LYP+D3/6-31+G** level. The solvent effect of tetrahydrofuran (THF) was considered by using PCM method. Gaussian16 package was used.

【Results】

The energy diagram of the dissociation reaction of N_2 on Li_{25} clusters is shown in **Fig. 1**. The reaction barrier for N_2 dissociation on Li_{25} clusters was 149.2 kJ/mol, while the dissociation energy of the N≡N triple bond in vacuum is about 945 kJ/mol. From these results, the Li cluster would facilitate the dissociation of N_2.

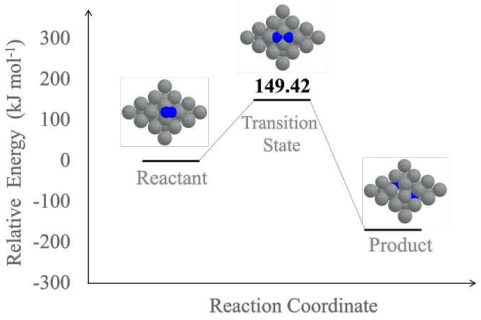

Fig. 1 The energy diagram of the dissociation reaction of N_2 on the Li_{25}.

Additionally, the reaction barrier tended to decrease with the increasing number of hydrogen atoms added to the N_2 molecule. In the case of three hydrogen atoms are added to N_2, the dissociation reaction occurs with no barrier. We also found that the charge of the system and the cluster size affect the reaction barrier.

References

1. M.S. Iqbal et al., **Ind. Chem. Mater**, *1*, 563-581 (2023).
2. H.L. Du et al., **Nature**, *609*, 722-728 (2022).

Resource theory of non-steerability-breaking channel

Chao-Hsien Wu[1], Chung-Yun Hsieh[2], Huan-Yu Ku*[1]
1. Department of Physics, National Taiwan Normal University, Taipei 11677, Taiwan
2. H. H. Wills Physics Laboratory, University of Bristol, Tyndall Avenue, Bristol, BS8 1TL, UK
Email: huan.yu@ntnu.edu.tw

ABSTRACT
Quantum steering, crucial for quantum advantages in one-sided (1S) device-independent (DI) quantum information tasks, can be enhanced via local filters, leading to stochastic steering distillation. This enhancement can be employed to distill entanglement and improve the quality of, for instance, 1SDI quantum key distribution. Due to the inevitable interaction between the system and its environment, steerability may degrade to unsteerability. In this work, we develop a resource theory for non-steerability-breaking channels. We define the free operations within this resource theory, revealing that they are equivalent to the free operations of the resource theory of quantum memory (characterized by entanglement-breaking channels). This suggests a direct connection between steerability breaking and entanglement-breaking channels. We then introduce the concept of robustness for non-steerability-breaking channels and demonstrate that it serves as a valid monotone within the framework of the resource theory. Furthermore, we show that non-steerability-breaking channels can be both distilled and activated stochastically within this theoretical framework.

References
1. H.-Y. Ku, J. Kadlec, A. Černoch, M. T. Quintino, W. Zhou, K. Lemr, N. Lambert, A. Miranowicz, S.-L. Chen, F. Nori, and Y.-N. Chen, **Quantifying Quantumness of Channels Without Entanglement**, *PRX Quantum* **3**, 020338 (2022).
2. D. Rosset, F. Buscemi, and Y.-C. Liang, **Resource Theory of Quantum Memories and Their Faithful Verification with Minimal Assumptions,** *Phys. Rev. X* **8**, 021033 (2018).
3. H.-Y. Ku, K.-Y. Lee, P.-R. Lai, J.-D. Lin, and Y.-N. Chen, **Coherent activation of a steerability-breaking channel**, *Phys. Rev. A* **107**, 042415 (2023).
4. H.-Y. Ku, C.-Y. Hsieh, S.-L. Chen, Y.-N. Chen, and C. Budroni, **Complete classification of steerability under local filters and its relation with measurement incompatibility**, *Nat Commun* **13**, 4973 (2022).

Analytically estimate quantum steering robustness of pure entangled state

Mao-Ting Wen[1], Shin-Liang Chen[2], Chia-Yi Ju[3] and Huan-Yu Ku[1]*

1. Department of Physics, National Taiwan Normal University
2. Department of Physics, National Chung Hsing University
3. Department of Physics, National Sun Yat-Sen University

e-mail: huan.yu@ntnu.edu.tw

ABSTRACT

Quantum steering, proposed by Einstein, Podolsky and Rosen in 1935, refers to the fact that in a bipartite quantum system, one party (Alice) can "steer" the quantum state of another party (Bob) through Alice's local measurements. Steering robustness is one of the typical quantifications in quantum steering. Although the steering robustness can be numerically computed by a classical algorithm, a semidefinite program, an analytic result of steering robustness is studied less. Here, we consider the simplest scenario; namely a pure entangled state $|\psi\rangle = \cos\theta\ |00\rangle + \sin\theta\ |11\rangle$ sharing between Alice and Bob. By analyzing the constraints and numerical solutions from semidefinite programming, we reduce the required parameters in solving the analytic solutions of steering robustness for pure entangled states. Then, we apply the Lagrange multiplier method to numerically construct a solution with a given θ. It is highly possible to derive the analytical solution of the steering robustness with a given θ for a pure entangled state. In this poster, we provide the overview of estimating the relationship between parameters in solving steering robustness, and a given θ from a pure entangled state.

References

1. D. Cavalcanti and P. Skrzypczyk. Quantum steering: a review with focus on semidefinite programming, Rep. Prog. Phys. **80** 024001 (2017)

Systematic Analysis of Positron Binding to Halogenated Hydrocarbons

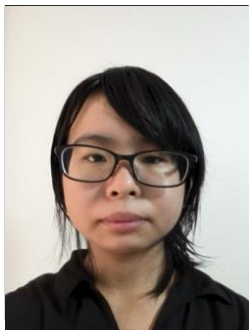

Miu Ashiba[1*], Daisuke Yoshida[2], Yukiumi Kita[1], and Masanori Tachikawa[1]

[1] Graduate School of NanoBioScience, Yokohama City University, 22-2 Seto, Kanazawa-Ku, Yokohama 236-0027, Kanagawa, Japan

[2] Nuclear Theory Group, Department of Physics, Tohoku University, Aramaki Aza-Aoba 6-3, Aoba-ku, Sendai 980-8578, Japan

[*] n245201f@yokohama-cu.ac.jp

ABSTRACT

A positron, the antiparticle of an electron with a positive charge, is now used in detecting cancer cells and lattice defects, but detailed properties remain unknown at the atomic/molecular level. Recently, Green *et al*. have theoretically demonstrated the positron binding to small halogenated hydrocarbons with *ab inito* many-body theory developed by them [1]. More comprehensive and systematic investigations, however, are indispensable in revealing the effect of halogenation on the positron binding to hydrocarbons in detail. In this study, to clarify the relationship between halogen atoms and positron binding, we theoretically analyzed the positron binding to halogenated hydrocarbons, $C_lH_mX_n$ (l=1~3,m+n=4,X=F,Cl,Br), using the positron-electron correlation-polarization potential (CPP) approach [2] developed by Takayanagi *et al*.

Figure 1 shows the surface of the constant density of the positron attached to CH_3F; the binding energy of the positron is 5.5 meV. The attached positron is mainly distributed around the fluorine atom. This is due to the attractive interaction between the positron and negatively charged fluorine atom; the net charge of the fluorine atom is -0.44190. Such a trend of the attached positron is also consistent with the results of the positron orbital of CH_3Cl reported by Green *et al*. Further details and results for other molecules will be presented on the day.

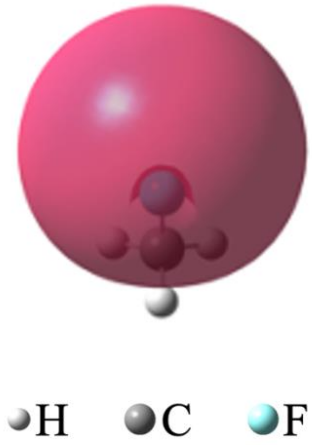

Figure 1: the constant density surface of the positron attached to CH_3F.

References

1. J. S. Green and R. G. Miller, *Phys. Rev. A*, **109**, L040801 (2024)
2. Y. Sugiura, H. Suzuki, T. Otomo, T. Miyazaki, T. Takayanagi, and M. Tachikawa, *J. Comp. Chem*., **41**, 1576-1585 (2020)

Exceptional Topological Phase Transition in an Optical Mirror

Tian-Shu Gou[1,3,*], Yi-Cheng Wang[2], Jhih-Shih You[5], and Hsiang-Hua Jen[3,4]

[1]*Department of Physics, National Taiwan University, Taipei 10617, Taiwan*
[2]*Department of Physics, University of California, Berkeley, California 94720, USA*
[3]*Institute of Atomic and Molecular Sciences, Academia Sinica, Taipei 10617, Taiwan*
[4]*Physics Division, National Center for Theoretical Sciences, Taipei 10617, Taiwan*
[5]*Department of Physics, National Taiwan Normal University, Taipei 11677, Taiwan*
*tianshugou@gmail.com

ABSTRACT

Recent studies of light-matter interactions in two-dimensional atomic arrays with subwavelength spacings have shown various interesting phenomena in quantum optics and topology [1,2]. However, the non-Hermitian part of the topic has yet to be thoroughly explored. The non-Hermiticity within the light cone has predicted the appearance of exceptional points (EPs) when symmetry in lattice geometry is lowered and the emergence of geometry-dependent non-Hermitian skin effect [3].

In this work, we study the non-Hermitian characteristics of a two-dimensional atomic array with long-range dipole-dipole interactions under the influence of lattice geometry and magnetic field. By considering a continuous deformation between the triangular and square lattice while preserving the atomic spacing as shown in Fig. 1, we discover that the exceptional points indeed emerge inside the light cone during the process. Furthermore, by calculating complex energy bands and associated Chern numbers, we obtain the phase diagram of the atomic array as a function of deformation strength η and magnetic field magnitude B in Fig. 2. We find that the emergence of topological phase (triangular lattice) and trivial phase (square lattice) that are separated by a gapless phase with EPs, which are robust against any finite magnetic field when $\eta_{c1} < \eta < \eta_{c2}$. Apart from the geometry-dependent skin effect for the bulk modes, the interplay of non-Hermiticity and topology can lead to geometry-dependent skin-topological edge modes in finite-size atomic arrays.

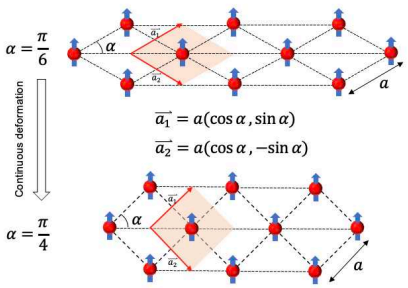

Fig. 1. Continuous deformation between triangular and square geometries with constant atomic spacing.

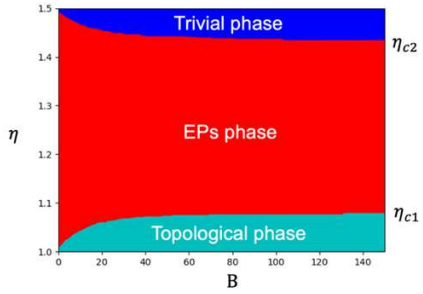

Fig. 2. Topological phase diagram of a 2D atomic array. (Deformation strength $\eta = 6\alpha/\pi$).

References

[1] Shahmoon, E., Wild, D. S., Lukin, M. D. & Yelin, S. F. Phys. Rev. Lett. 118, 113601 (2017).
[2] Perczel, J. et al. Phys. Rev. Lett. 119, 023603 (2017).
[3] Y.-C. Wang, J.-S. You, and H. H. Jen. Nat. Commun. 13, 4598 (2022).

Theoretical clarification of H/D isotope effects on the phase transition temperature of $K_3H(SO_4)_2$

Yuu Ishii, Kazuaki Kuwahata, Tomomi Shimazaki, and Masanori Tachitawa

Yokohama City University, Japan

n235202c@yokohama-cu.ac.jp

ABSTRACT

$K_3H(SO_4)_2$ (KHS) crystal is one of the hydrogen-bonded dielectrics (Figure 1). KHS exhibits paraelectric phases at finite temperatures and does not undergo a phase transition. In contrast, $K_3D(SO_4)_2$ (KDS), in which hydrogen (H) is replaced by deuterium (D), shows a significant H/D isotope effect. KDS undergoes phase transition from paraelectric to antiferroelectric below the phase transition temperature Tc = 85 K [1]. However, the molecular-level understanding of the H/D isotope effect on this phase transition temperature is not yet fully understood. Therefore, the purpose of this study is to elucidate the mechanism of the KHS phase transition and its isotope effect using theoretical calculations. Investigating the isotope effect requires a method that can distinguish between hydrogen and deuterium atoms. Therefore, we employed the path integral molecular dynamics (PIMD) method [2], which can account for the nuclear quantum effect. The PIMD simulations were performed for KHS and KDS to reveal the isotope effect.

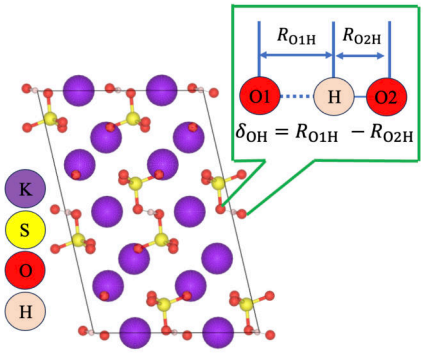

Figure 1. Crystal structure of KHS and the definition of δ_{OH}

Results &Discussion

Figure 2 shows the free energy surface along with the hydrogen bond direction and the thermal kinetic energy ($1/2k_BT$) under 300 K and 50 K. At 300 K (Figure 2(a)), the barrier energies of Qm (H) and Qm (D) are both lower than the thermal kinetic energy of 300 K, indicating the H and D atoms are free to move between the two stable points. The barrier of Qm (H) at 50 K is still lower than the thermal kinetic energy, while that of Qm (D) is higher. This suggests that the D atoms cannot cross the barrier, are expected to be localized, and undergo a phase transition to antiferroelectric. The detailed discussion will be presented on the day.

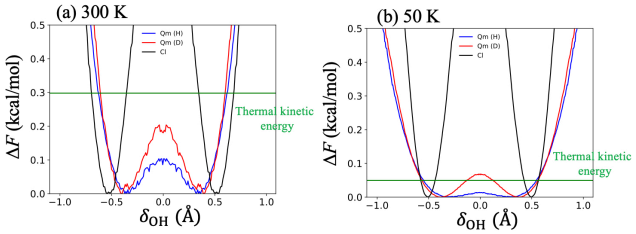

Figure 2. Free energy surface as a function of δ_{OH} and the kinetic energy at (a) 300 K and (b) 50 K

References

[1] Y. Noda, H. Kasatani, Y. Watanabe, and H. Terauchi, *J. Phys. Soc. Jpn.* **61**, 905 (1992).

[2] M. Shiga, M. Tachikawa, and S. Miura, *J. Chem. Phys*. **115**, 9149 (2001).

Time-domain Measurement-based quantum computation on cloud computer

Po-Yang Chen,[1] Zhi-Peng Yang,[234] Franco Nori,[345] Huan-Yu Ku*,[1]

[1]Department of physics, National Taiwan Normal University
[2]Beijing Academy of Quantum Information Science, Beijing, China
[3]Theoretical Quantum Physics Laboratory, RIKEN Cluster for Pioneering Research, Wako-shi, Saitama Japan
[4]Center for Quantum Computing, RIKEN, Wako-shi, Saitama Japan
[5]Department of Physics, The University of Michigan, Ann Arbor, Michigan, USA
huan.yu@ntnu.edu.tw

As one of the approaches to achieve universal quantum computation, measurement-based quantum computation (MBQC) uses measurements on a large-entangled state (cluster state) and single qubit corrections. However, physically generating large-scale cluster states remains challenging due to the decoherence and the complexity of required operations on the system. To reduce the complexity of a linear cluster state preparation, here, we recycle the measured single qubit in MBQC model, enabling us to construct N numbers of an entangled state with merely *two* qubits. We call this approach as time-domain cluster state generation. Then, based on our method, we construct circuit models to demonstrate a time-domain one-way X-rotation gate and a time-domain one-way Hadamard gate with a reset function that reduce the complexities of the standard one-way X-rotation and Hadamard gates. Due to the precise circuit models, our results can be implemented in the current cloud quantum computer.

References

1. Raussendorf, D. E. Browne, and H. J. Briegel, Measurement-based quantum computation on cluster states, **Physical Review A 68**, 022312 (2003).
2. W. Asavanant, Y. Shiozawa, S. Yokoyama, B. Charoen- sombutamon, H. Emura, R. N. Alexander, S. Takeda, J. Yoshikawa, N. C. Menicucci, H. Yonezawa, and A. Fu- rusawa, Generation of time-domain-multiplexed two- dimensional cluster state, **Science 366**, 373 (2019)
3. Z.-P. Yang, H.-Y. Ku, A. Baishya, Y.-R. Zhang, A. F. Kockum, Y.-N. Chen, F.-L. Li, J.-S. Tsai, and F. Nori, Deterministic one-way logic gates on a cloud quantum

computer, **Phys. Rev. A 105**, 042610 (2022)

4. S. Shirai, Y. Zhou, K. Sakata, H. Mukai, and J.-S. Tsai, Generating time-domain linear cluster state by recycling superconducting qubits, arXiv:2105.08609(2021)

Laser-Induced Photoresponse in MoS_2-Based Optoelectronic Devices

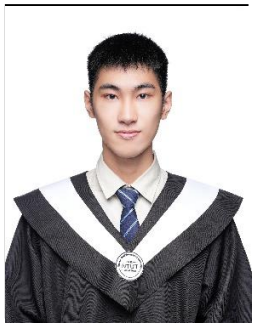

Cheng-Yu Huang[1,2], Yi-Chih Cheng[1,2], Jung-Chen Tung[1*], and Ting-Hua Lu[2*]

[1] Department of Electro-Optical Engineering, National Taipei University of Technology, Taipei, Taiwan

[2] Department of Physics, National Taiwan Normal University, Taipei, Taiwan

e-mail: t112658003@ntut.org.tw

ABSTRACT

Two-dimensional (2D) material semiconductors have demonstrated significant potential for use in photodetectors, optical switches, light emitters, and other optoelectronic devices. The unique combination of their electrical properties and optical characteristics under illumination enhances their performance in these applications.[1,2,3] In this work, we systematically analyze the photocurrent, on/off current ratio, and responsivity of MoS_2-based transistor by measuring the back-gate current and drain current under different 532 nm laser irradiation powers. We observed that with increasing laser power, the photocurrent is enhanced due to the rising density of free electron-hole pairs generated during interband transitions. Additionally, we noted that the on-off current ratio increases as the photocurrent rises. However, the responsivity is observed to decrease with the increase in laser power. Our findings provide the development of the high-performance optoelectronic devices based on MoS_2 and play an important role in future technological applications.

References

1. A. D. Bartolomeo, L. Genovese, F. Giubileo, L. Iemmo, G. Luongo, T. Foller and M. Schleberger. **2D Materials**, 5 ,015014 (2018).
2. J. Panda, S. Sahu, G. Haider, M. K. Thakur, K. Mosina, M. Velický, J. Vejpravova, Z. Sofer, and M. Kalbác. **ACS Appl. Mater. Interfaces**, *16, 1*, 1033–1043 (2024).
3. Y. J. Feng, K. B. Simbulan, T. H. Yang, Y. R. Chen, K. S. Li, C. J. Chu, T. H. Lu, and Y. W. Lan. **ACS Nano**,*16, 6*, 9297–9303 (2022)

Iterative synthesis of long-chain polyamines (LCPAs) with diverse chain lengths to elucidate their cell-penetrating activities

Taiga Ohnishi, Raku Irie, Masato Oikawa
Yokohama City University
e-mail: n245206d@yokohama-cu.ac.jp

ABSTRACT

Aculeines (ACUs) are polyamine-peptide-conjugated marine natural products that exhibit potent cytotoxicity by penetrating cell membranes and entering the nucleus.[1,2] A fluorescently labeled long-chain polyamine (LCPA, 12-mer), previously synthesized in our laboratory, thereafter showed that it also penetrates the plasma membrane of the HeLa cell and enters the nucleus. This observation suggested that the cell membrane permeability of ACUs is conferred by LCPA. In this study, the author planned to synthesize LCPAs with diverse chain lengths to elucidate the relationships between the chain length and the cell-penetrating activity of LCPAs.

By developing the split-couple strategy, 7-mer polyamine **4** was successfully synthesized from 3-mer polyamine **1**. By iteratively applying the established strategy to **4** thus synthesized, even longer polyamines (11-mer and 15-mer) were synthesized.

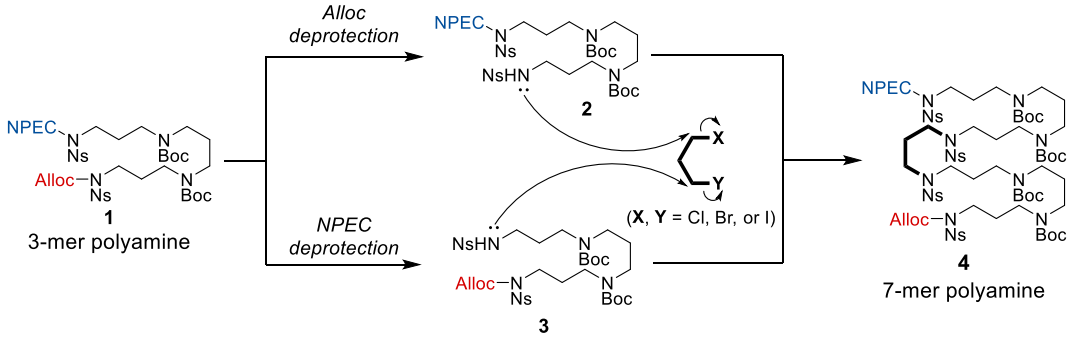

The author's other efforts to prepare fluorescently labeled LCPAs to explore locations in the HeLa cell will also be presented.

References

1. Matsunaga S. et al., **ChemBioChem**, *12*, 2191–2200 (2011).
2. Watari H. et al., **Chem. Lett.**, *52*, 185–189 (2023).

Development of a Portable Instrument for Laser-Assisted Microscopic Analysis of Materials

Shih-Chieh Chen, Yu-Chen Chang, Ting-Hua Lu
Department of Physics, National Taiwan Normal University, Taiwan
Email: qwe0956584768@gmail.com

ABSTRACT

The goal is to develop an instrument capable of integrating a nanoscale thin film material imaging system with a laser irradiation system during the measurement process. This device will offer the flexibility to investigate surface interactions including optical and electrical properties of samples. Our homemade optical imaging system, which features a portable and movable platform, will be adaptable to various light sources and samples. Additionally, by incorporating a grating and a high-resolution CCD, it will capture scattered light and the emitted spectrum from the sample. We have successfully employed this home-made instrument to measure the photoluminescence spectra of MoS_2 and commercial Rhodamine. This achievement demonstrates that the protable system can analyze both photoluminescence (PL) and Raman characteristics, offering new opportunities for exploring additional physical properties of optoelectronic devices.

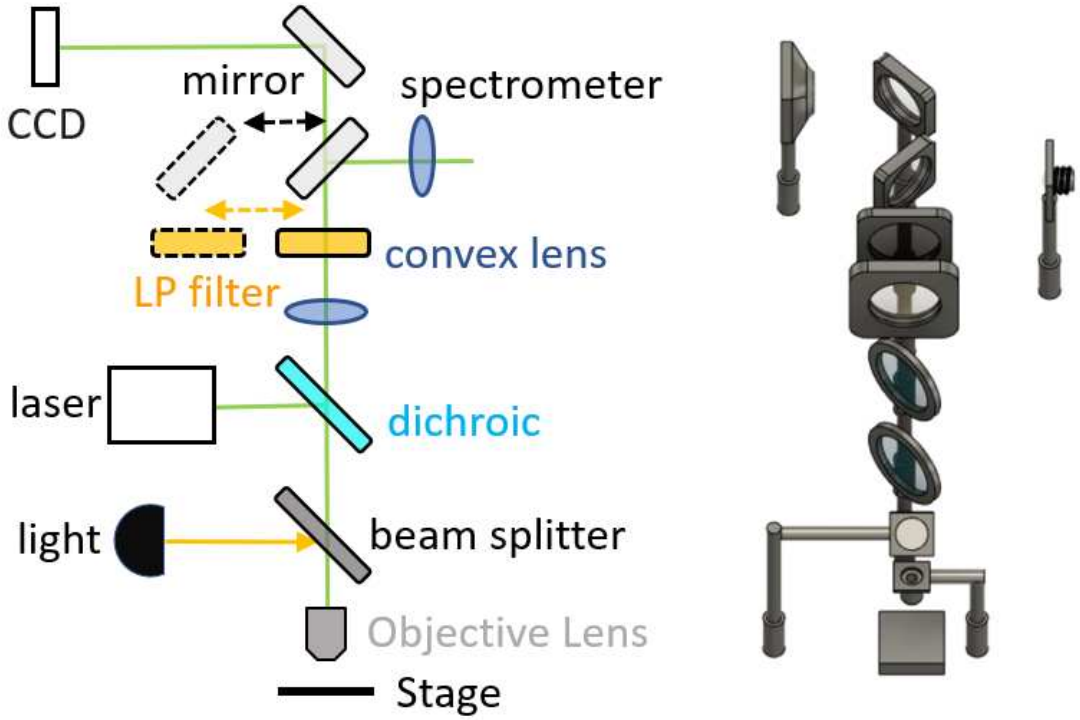

Figure 1. Microscopic experimental setup, including a movable and portable CCD and Laser-assisted imaging system.

Negative-Ion Mass Spectrometry of Ibuprofen and Its Analogues

H.Nagata, K.Sekimoto
Graduate School of Nanobioscience, Yokohama City University
n245217a@yokohama-cu.ac.jp

ABSTRACT

Ibuprofen, a component of antipyretic analgesics, is an aromatic compound with a carboxyl group and is known to exist as ions in vivo. Since many pharmaceuticals contain carboxyl groups, it is expected that understanding the ion structures and stability of ibuprofen will contribute to develop pharmaceutical research. In this study, we measured ibuprofen and its analogues (aromatics with a carboxylic group) using an atmospheric pressure corona discharge ionization collision-induced dissociation mass spectrometry (APCDI-CID-MS) in negative-ion mode. Also, we performed CID experiments on deprotonated molecules for individual analytes. As a result, it was found that there are two conditions to form negative ions with only C and H atoms: (1) stabilization by forming a double bond by 2H loss and broadening the resonance structure, so making it possible to eliminate CO_2 (Fig. 1a), and (2) stabilization by forming a benzyl anion at the α carbon of a carboxyl group or a methyl group via CO_2 loss (Fig. 1b).

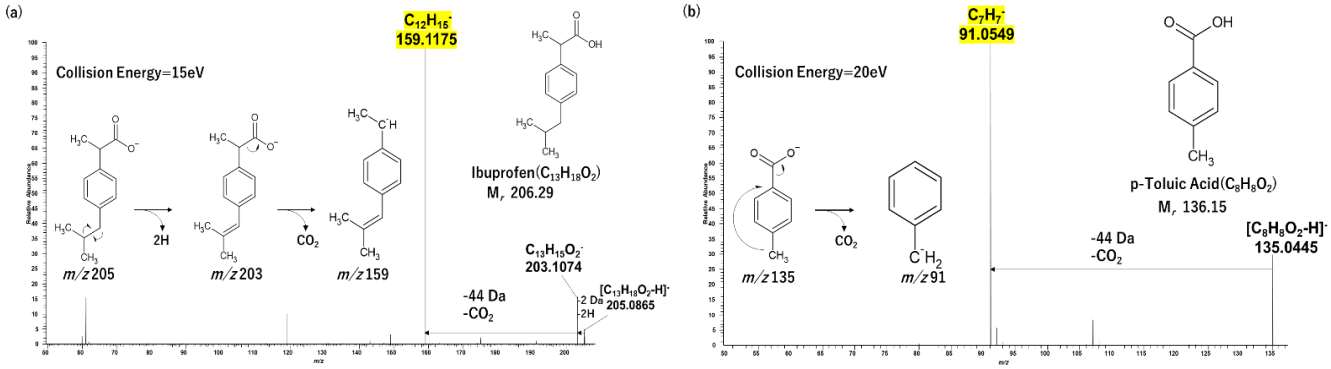

Fig.1. CID spectra of (a) deprotonated ibuprofen $[C_{13}H_{18}O_2\text{-}H]^-$ and (b) deprotonated p-toluic acid $[C_8H_8O_2\text{-}H]^-$

References

1. K. Sekimoto, M. Takayama, Eur. Phys. J. D, 60, 589-599 (2010)
2. Mary L. Bansu, Kathryn R. Watkins, Melinda L. Bretthauer, Christopher A. Moore, and Heather Desaire. *Anal. Chem*. **76,6**, 1746-1753(2004)
3. M. Farre, M. Petrovic & D. Barcelo. *Analytical and Bioanalytical Chemistry*. **387**, 1203-1214(2007)

Enhanced Stability of Gr/MoS_2 and h-BN/MoS_2 Heterostructures under Laser Illumination

Hsin-Sung Chen, Chak-Ming Liu, Sheng-Yu Hsu, Chuan-Che Hsu, Yann-Wen Lan, Hsiang-Chih Chiu, Wen-Chin Lin*
Department of Physics, National Taiwan Normal University
e-mail: wclin@ntnu.edu.tw

ABSTRACT

Its limited thickness and vulnerability challenge the optical measurement of molybdenum disulfide (MoS_2) to damage by high-intensity laser illumination, which can cause severe local heating and structural degradation. To address this, materials with high thermal conductivity and transparency, such as graphene (Gr) and hexagonal boron nitride (h-BN), are proposed as protective layers. This study employs Raman and photoluminescence (PL) spectroscopy to monitor the stability of bare MoS_2 flakes and MoS_2 flakes covered with either Gr or h-BN under varying laser powers in real time. When exposed to a high laser power density for 30 minutes, bare MoS_2 shows significant structural degradation, with protrusions forming and the Raman signal decreasing to just 10% of its initial intensity. Conversely, in the Gr/MoS_2 heterostructure, both the Raman fingerprint peaks and PL intensity remain stable with only 0-10% reduction, indicating effective thermal dissipation through the Gr cover layer. The h-BN/MoS_2 system also demonstrates enhanced stability, and the Raman signal decreases to around 30% of its initial intensity. These findings suggest that the Gr/MoS_2 system offers the highest stability under laser illumination, followed by the h-BN/MoS_2 system, whereas bare MoS_2 exhibits the lowest stability.

Synthetic studies of Scopadulciol, a novel anticancer drug lead compound

Ibuki Ozawa, Yuichi Ishikawa
Graduate School of Nanobioscience Yokohama City University
e-mail: n235207a@yokohama-cu.ac.jp

ABSTRACT

The Wnt signaling pathway regulates cell proliferation and differentiation, and its abnormal activation causes proliferation of human cancer cells. Scopadulciol (**Figure1**) is a compound isolated from the tropical native plant *Scoparia dulcis*, which exhibits inhibitory activity against the Wnt signaling pathway.[1] Although, it is expected as a novel anticancer drug lead compound, the detailed mechanism of activity has not been reported. We started this study to develop an efficient synthetic method for Scopadulciol and to elucidate the detailed mechanism of activity.

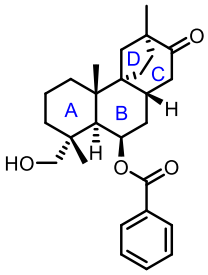

Figure 1 Scopadulciol

To date, the intermediates **3** was obtained in 31% yield from (*3aR*)-(+)-Sclareolide (**1**). As future plan, after the acetal protection of compound **4** the C, D-ring, the synthesis of Scopadulciol will be achieved (**Scheme1**).

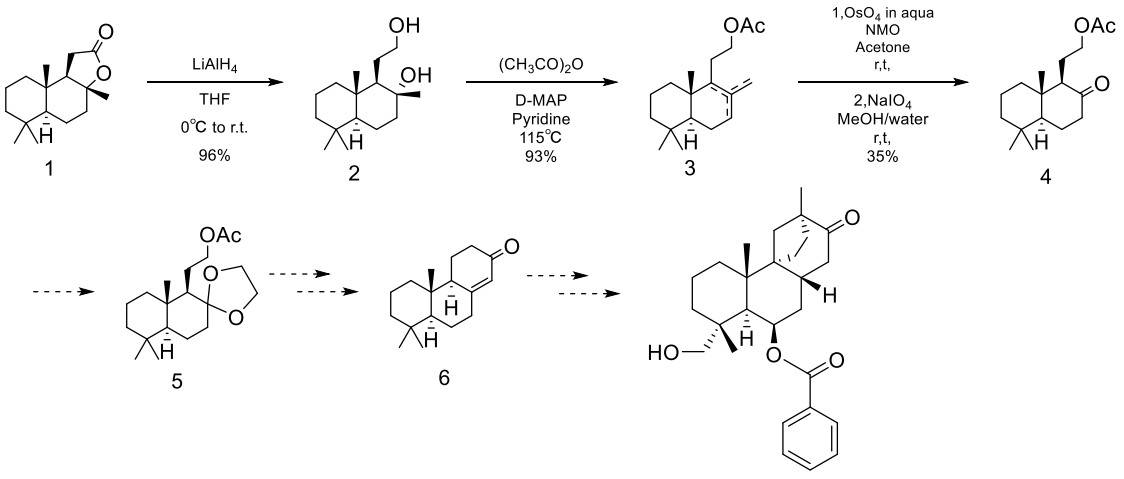

Scheme 1

Reference

1. R. G. Fuentes, K. Toume, M. A. Arai, S. K. Sadhu, F. Ahmed, M. Ishibashi, *J. Nat. Prod.* **2015,** 78, 864-872.

Optical properties of the extract of annealed C_{60} NWs

Juri Miyamoto, Yuto Sakai, Yota Katada, Ken Inoue, Ryo Suzuki and Masaru Tachibana
Graduate School of Nanobioscience, Yokohama City University, Japan
e-mail: n245225b@yokohama-cu.ac.jp

ABSTRACT

Carbon Dots (CDs) are fluorescent carbon nanoparticles with diameters in the range of a few nanometers [1]. To synthesize CDs with uniform particle size, starting material is important. Fullerene C_{60} is favorable molecule for starting material due to its well-defined dimension. It has been reported that CD can be synthesized by decomposing C_{60} using strong acids and oxidizers [2]. However, this method involves tedious synthetic procedures. In our laboratory, we synthesize fiber-like C_{60} crystals called C_{60} nanowhiskers (C_{60} NWs) [3]. Recently, we found that the cages of C_{60} molecules in C_{60} NWs can be broken by annealing at 300°C in air. In this study, we examine the synthesis of CDs solely through annealing of C_{60} NWs.

C_{60} NWs are grown using the Liquid-liquid interfacial precipitation method [4]. The Raman spectra of pristine and annealed C_{60} NWs are shown in Fig.1. The sharp peaks observed in the pristine C_{60} NWs are derived vibrational modes of C_{60} [5]. After annealing, however, these peaks disappeared and new peaks originating from amorphous carbon appeared [6]. This indicates destruction of C_{60} cages and synthesized amorphous carbon. Both pristine and annealed NWs were dispersed in pyridine solution. The photographs of pristine and annealed C_{60} NWs solution under white light and UV light are shown in Fig. 2. The pristine solution did not exhibit luminescence under UV light, while annealed C_{60} NWs solution exhibited luminescence under UV light. We get the fluorescence spectra of the pristine and annealed C_{60} NWs solution at an excitation wavelength of 380 nm. The annealed C_{60} NWs solution exhibited a new fluorescence peak, at a longer wavelength compared to the pristine solution, potentially originating from the broken C_{60} cages. This suggests the possibility that CDs were formed.

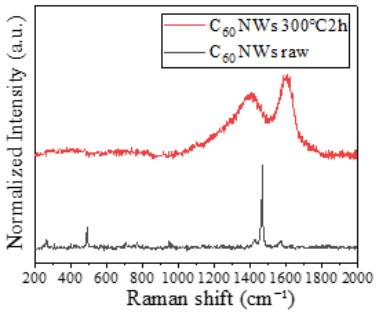

Fig. 1 Raman shift of pristine and annealed C_{60} NWs

Fig. 2 pristine and annealed C_{60} NWs solution

References

1. S. N. Baker, *et al*., **Angew. Chem. Int. Ed.**, *49*, 6726 (2010).
2. C. K. Chua *et al.,* **ACS Nano**, *9* (3) 2548 (2015).
3. Y Funamori *et al*., **Carbon**, *169*, 65 (2020)
4. K. Miyazawa *et al.,* **J Mater. Res.**, *17*, 83 (2002)
5. A. M. Rao *et al*., **Science**, *259*, 955 (1993)
6. H. Ahalapitiya, *et al*., **Carbon**, *42*, 1143 (2004).

Direct CVD growth of $W_xTi_{(1-x)}S_2$ for Room-temperature layered ferromagnetic materials

Kai-Wen Hsiao[1, 2], Yu-Xiang Chen[2], Yann-Wen Lan[1], Ya-Ping Hsieh[2]

[1]Department of physics, National Taiwan Normal University, Taiwan
[2]Institute of Atomic and Molecular Sciences, Academia Sinica, Taiwan
e-mail: kevin43480@gmail.com

ABSTRACT

Ferromagnetic two-dimensional materials are crucial for advancing spintronics, magnetic sensors, and energy-efficient electronics, offering opportunities significant for semiconductor technology. In this study, we synthesize titanium-doped tungsten disulfide (Ti-doped WS_2) using chemical vapor deposition (CVD) to investigate the impact of Ti doping on the magneto-optical properties of WS_2. Although WS_2 lacks magnetism, the system gains ferromagnetic (FM) properties after Ti doping[1]. This magnetic transformation is a result of an altered charge density distribution in WS_2, resulting in its newfound magnetic behavior. Notably, this magnetic characteristic is stable at room temperature (~300K), opening up exciting possibilities in the field of valleytronics.

References

1. Xu Zhao, Congxin Xia...**Electronic and magnetic properties of X-doped (X = Ti, Zr, Hf) tungsten disulphide monolayer**, Journal of Alloys and Compounds, 654, 574-579 (2016).

Crystallization and evaluation of Thaumatin crystals with L-, D- tartrate

Takumi Oriyama, Ryo Suzuki, Masaru Tachibana
Graduate school of Nanobioscience, Yokohama City University, Japan
e-mail n245208f@yokohama-cu.ac.jp

ABSTRACT

The three-dimensional (3D) structures of protein molecules are important for the understanding biological phenomena and drug discovery. Protein crystal is generally used for X-ray diffraction structure analysis to determine the 3D structures of protein molecules. Since the accuracy of structural analysis depends on the quality of single crystals, high-quality protein crystals are necessary. Protein crystals are obtained by adding salt to reduce solubility and promote crystallization. Even for the same species of protein, the crystal structure changes depending on the type of salt used. Therefore, the effect of salt on crystal growth is one of the important factors. And more, proteins are chiral molecules composed of amino acids. It is expected that chiral salts would affect protein crystallization.

Herein, we focused on thaumatin, which is one of the protein molecules. It is known that Thaumatin can be crystallized by using tartrate [1]. Tartaric acid is a typical chiral molecule with in three forms: L-form, D-from and meso-compound. The thaumatin crystals were crystallized with L-tartaric acid at 0.2 M and 0.5 M, and with D-tartaric acid at 0.2 M and 0.5 M, via hanging drop technique.

As shown in Fig. 1(a, b), at a salt concentration of 0.2 M, crystals of about 500 μm in size were obtained when L-tartaric acid was used, but no crystals were obtained when D-tartaric acid was used. However, at a salt concentration of 0.5 M, crystals of about 500 μm in size were obtained when D-tartaric acid was used, but so many small crystals were crystallized when L-tartaric acid was used (Fig. 1 (c, d)). When protein crystals are grown, the protein solution must be supersaturated. The lower the solubility of the protein, the higher the degree of supersaturation. In general, higher supersaturation increases the frequency of crystal nucleation. At the same salt concentration, the solubility of thaumatin is lower with L-tartaric acid than with D-tartaric acid [1]. In the presentation, we discuss the crystallization details and the characterization of the crystals by X-ray diffraction.

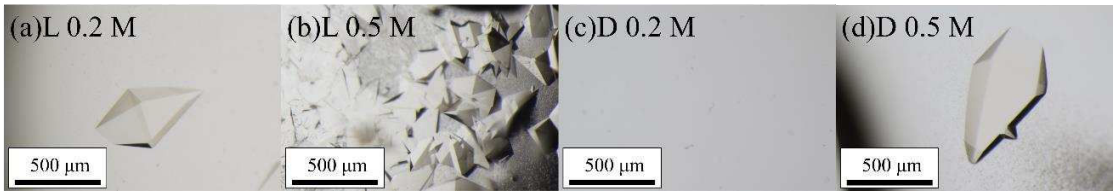

Fig. 1 Thaumatin crystals crystallized with (a) 0.2 M L-tartaric acid,
(b) 0.2 M D-tartaric acid, (c) 0.5 M L-tartaric acid and (D) 0.5 M D-tartaric acid

References

1. N. Asherie, *et al*., **Cryst. Growth Des.**, *8*, 1815 (2008).

Scanning Tunneling Luminescence measurements on C_{60} molecular films

L. Ogata[A, B], K. Kimura[A], K. Mochizuki[A, C], I. Katayama[D], H. Imada[A], T. Yokoyama[B], J. Takeda[D], Y. Kim[A, B]

[A]RIKEN SISL, [B]Yokohama City Univ.,
[C]Univ. of Tokyo, [D]Yokohama National Univ.
e-mail: n245207e@yokohama-cu.ac.jp

ABSTRACT

Fullerene (C_{60}) molecule is one of the typical n-type organic molecules and has been widely used for organic photovoltaics[1]. Since exciton dynamics in molecular films and at interfaces governs the properties of devices, it is important to study exciton dynamics on their intrinsic length scale. Optical spectroscopy based on scanning tunneling microscopy (STM) enables to investigate the exciton dynamics with atomic or molecular scale spatial resolution[2]. In this study, we prepared C_{60} molecular films on NaCl ultrathin insulating films grown on Au(111) and conducted electroluminescence measurements using STM.

Fig. 1(a) shows an STM image of C_{60} molecular films. In the STM image, C_{60} molecules are arranged in a close-packed structure and show three different topographic features depending on the orientations of C_{60} molecules. We labeled them A, B, and C as shown in Fig. 1(a) and assigned as hexagon (h), hexagon-pentagon (h:p), and hexagon-hexagon (h:h), respectively, considering the upward structures[3].

Fig. 1(b) shows scanning tunneling luminescence (STL) spectra measured on these three molecules. Several sharp peaks appeared in the STL spectra. These emissions originate from the excited states of the C_{60} molecules, and we found that their wavelengths depend on the orientations.

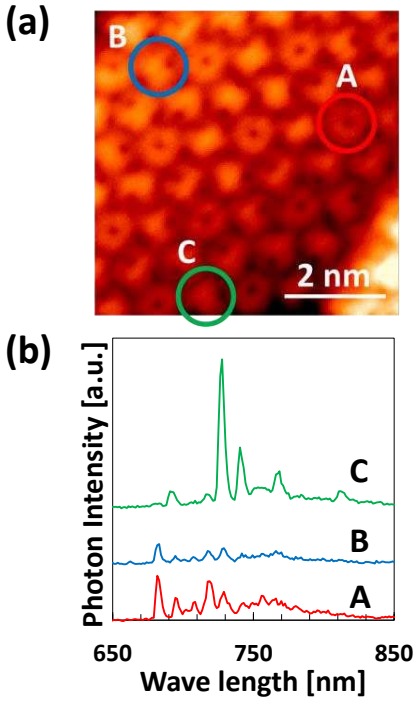

Fig. 1 (a) STM image of C_{60}/NaCl/Au(111) (3 pA, -2.7 V). (b) STL spectra obtained at the points in (a) (-3 V, 10 pA, 60 sec.).

References

1. K. Ozawa, S. Yamamoto, T. Miyazawa, K. Yano, K. Okudaira, K. Mase, I. Matsuda, **J. Phys. Chem. C**, *125*, 13963 (2021).
2. P. Merino, C. Groβe, A. Roslawska, K. Kuhnke, K. Kern, **Nat. Common**, *6*, 8461 (2015).
3. F. Rossel, M. Pivetta, F. Patthey, E. Cavar, AP. Seitsonen, WD. Schneider, Phys. Rev. B, **84**, 075426 (2011).

Surface characterization and control of skyrmions in van der Waals ferromagnet Fe_3GaTe_2

Ming-Hsien Hsu[1], Chak-Ming Liu[1], Po-Wei Chen[1], Po-Chun Chang[3,4], Masahiro Haze[2], Yixi Su[3], Yukio Hasegawa [2], Hsiang-Chih Chiu[1], Wen-Chin Lin[1*]

[1]National Taiwan Normal University, Taipei 11677, Taiwan

[2]Institute for Solid State Physics, the University of Tokyo, Chiba, 277-8581 Japan

[3] Jülich Centre for Neutron Science at Heinz Maier-Leibnitz-Zentrum, Forschungszentrum Jülich GmbH, Lichtenbergstr. 1, 85747 Garching, Germany

[4] Tamkang University, New Taipei 25137, Taiwan

[*]e-mail: wclin@ntnu.edu.tw

Magnetic skyrmions in two-dimensional (2D) van der Waals (vdW) ferromagnets demonstrate potential for high-density and low-energy-consumption spintronic devices. Most of the vdW ferromagnet Curie temperatures are below room temperature (RT). However, Fe_3GaTe_2 exhibits high Curie temperature above RT and large perpendicular magnetic anisotropy, as shown in Fig.1(a). In the present study, there are two methods for the observation of magnetic domain transitions. First, the magnetic domains undergo a transition from strip domains to skyrmions via laser-localized heating. In addition, an electric current caused local heating through conductive atomic force microscopy (CAFM), and we demonstrated the transition from strip domains to circular domains, as shown in Fig. 1(b). These phenomena reveal that local heating by laser illumination or CAFM could control the appearance of skyrmions. Figure 1(c) shows the topography of Fe_3GaTe_2 bulk using a low-temperature scanning tunneling microscope. A repetitive triangular pattern corresponding to the arrangement of Te atoms in the top layer of its four-layer structure is observed. The defects within these triangular structures may be due to the presence of Fe_I atoms in the second layer. These findings offer valuable insights for future magnetic and structural research.

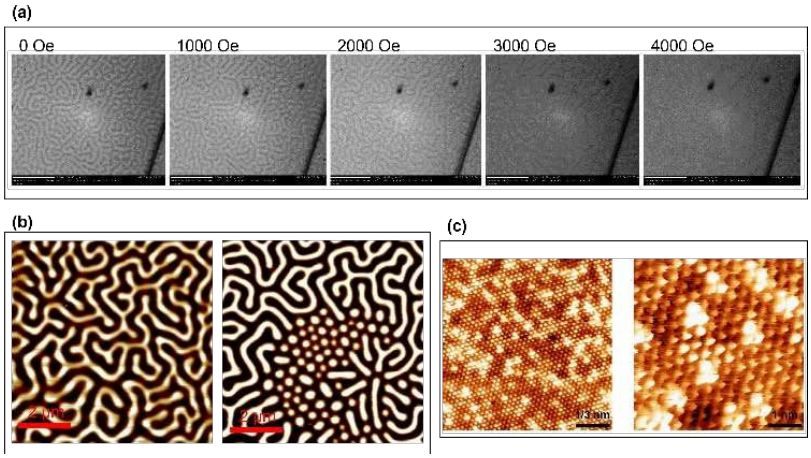

Fig. 1 (a) Magneto-optical Kerr images show field-dependence of the magnetic domain structure on a Fe_3GaTe_2 crystal surface. (b) MFM images were scanned before and after applying local current by CAFM. (c) STM images were measured on an in-situ cleaved Fe_3GaTe_2 surface.

Measurements of coffee aromas using atmospheric pressure corona discharge ionization mass spectrometry

Momomi Morita, Kanako Sekimoto
Graduate School of Nanobioscience, Yokohama City University
e-mail: n245226c@yokohama-cu.ac.jp

ABSTRACT

Coffee aroma is made from Maillard reaction that occurs between amino acids and carbonyl compounds to produce colored products and flavor compounds.

Coffee aroma has a relaxing effect for human, but the magnitude of this effect is different between its variety. Previous research has shown that Guatemala has a high relaxing effect, while Mandarin has a relatively low relaxing effect[1]. In this study, we measured liquid coffee aromas for Guatemala and Mandarin and volatile compounds emitted during heating those beans pasted, using atmospheric pressure corona discharge ionization mass spectrometry (APCDI-MS). We will discuss which compounds are emitted and relationship with the Maillard reaction.

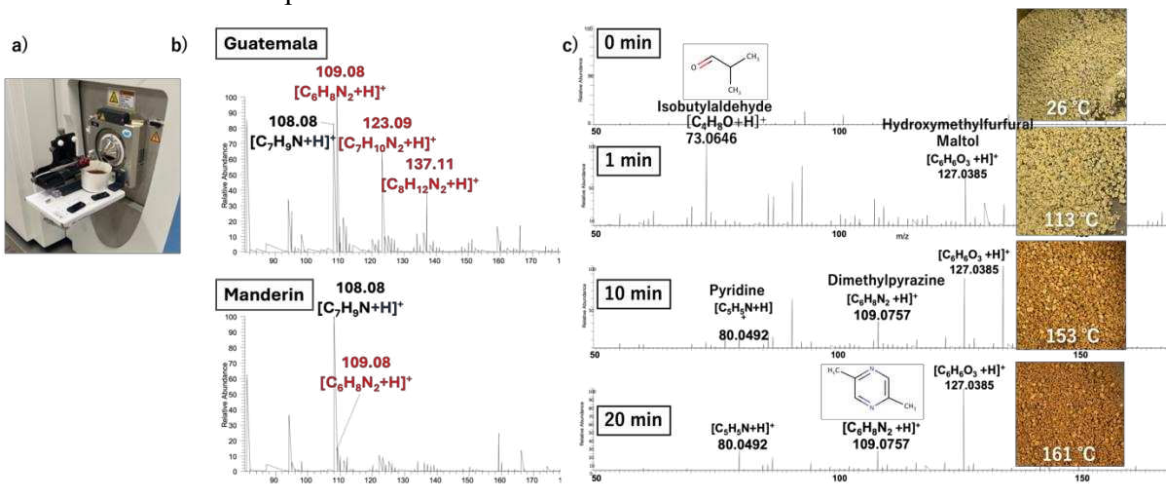

Figure 1 a) Measurements of liquid coffee aroma by APCDI-MS. b) APCDI-MS spectra of liquid coffee aroma. c) APCDI-MS spectra at 0, 1, 10, and 20 minutes during heating beans pasted.

References

1. Y.Koga. **Effects of Odors on Brain Function,** *International Society of Life Information Science, Vol.22, No.1*, 179-183 (2004).

Logically Derived Sequence Tandem Mass Spectrometry for Structural Determination of Unusual Complex N-glycan in Eggs

Min-Han Tsai[1,2], and Chi-Kung Ni[2,3*]

1.Department of Chemistry, National Taiwan Normal University, Taipei, Taiwan
2.Institute of Atomic and Molecular Sciences, Academia Sinica, Taiwan
3.Department of Chemistry, National Tsing Hua University, Hsinchu, Taiwan

e-mail: ktenleo@gmail.com

ABSTRACT

Carbohydrates play a crucial role in biology. While scientists have extensively studied the structures of proteins and nucleic acids, applying their findings practically, carbohydrates present a unique challenge due to their complex structures. To tackle this challenge, we developed a novel mass spectrometry technique known as LODES/MSn (Logical Derivatized Sequence Tandem Mass Spectrometry) for the structural identification of underivatized oligosaccharides. This method enables us to discern linkage positions, anomericity, and stereoisomers within oligosaccharides.

My research focuses on N-glycans, which are categorized into three types: high mannose, complex, and hybrid. N-glycans are closely intertwined with the metabolism of numerous organisms. Within the N-glycan biosynthetic pathway, it is theoretically expected that $Man_3GlcNAc_3$ would have only one possible configuration. However, I find multiple isomers present in both chicken egg whites and quail egg whites.

References

1. Jurgen T. Sanes, Hiroshi Hinou, Yuan Chuan Lee, and Shin-Ichiro Nishimura* Glycoblotting of Egg White Reveals Diverse N-Glycan Expression in Quail Species **J. Agric. Food Chem.** 2019, 67, 1, 531–540

2. Chengjian Wang, Meifang Yang, Xi Gao, Cheng Li, Zihua Zou, Jianli Han, Linjuan Huang & Zhongfu Wang The ammonia-catalyzed release of glycoprotein N-glycans **Glycoconjugate Journal** (2018) 35:411–420

Inspection on grain boundary structures of large-area molybdenum disulfide by spectroscopic mapping technologies

Min-Jia Zhang[1*], Yann-Wen Lan[1], Shao-Yu Chen[2,3]

[1]Department of Physics, National Taiwan Normal University, Taipei, Taiwan

[2]Center for Condensed Matter Sciences, National Taiwan University, Taipei, Taiwan

[3]Center of Atomic Initiativefor New Materials, National Taiwan University, Taipei, Taiwan

e-mail: 1218kaemi@gmail.com

ABSTRACT

Molybdenum disulfide (MoS_2) is increasingly important in the semiconductor industry. The attainment of large, wafer-scale monolayers of MoS_2 is crucial for improving device yield. By employing chemical vapor deposition (CVD) on miscut sapphire substrates, we successfully cultivated monolayer MoS_2 samples with substantial surface coverage and merged grains. However, some variations and grain boundaries persist among different crystals. To precisely determine the axial orientation of the crystal lattice, we utilized second harmonic generation (SHG) spectroscopy[1]. Furthermore, we implemented an SHG mapping system to examine the distribution of axial orientations and intrinsic strain in our samples[2]. When comparing SHG to photoluminescence spectroscopy (PL), we observed a greater magnitude in the PL signal, whereas the SHG signal at the boundaries displayed reduced symmetry and amplitude. This disparity in spectroscopic results warrants a more comprehensive investigation into the underlying mechanisms.

References

1. He, C., Wu, R., Zhu, L., Huang, Y., Du, W., Qi, M., Zhou, Y., Zhao, Q., & Xu, X. (n.d.). **Anisotropic Second-Harmonic Generation Induced by Reduction of In-Plane Symmetry in 2D Materials with Strain Engineering.**, J. Phys. Chem. Lett. 2022, 13, 352-361
2. Li, Y., Rao, Y., Mak, K. F., You, Y., Wang, S., Dean, C. R., & Heinz, T. F. (n.d.). **Probing Symmetry Properties of Few-Layer MoS_2 and h-BN by Optical Second-Harmonic Generation.** Nano Lett. 2013, 13, 3329-3333

Texture control to achieve high in-plane thermoelectric performance in polycrystalline tin monosulfide (SnS) co-doped with silver and sodium

M. Y. Fakhri, L. C. Chen, and K. H. Chen

International Graduate Program of Molecular Science and Technology (NTU-MST), National Taiwan University
Institute of Atomic and Molecular Sciences, Academia Sinica
Centre for Condensed Matter Sciences, National Taiwan University
e-mail: d08551006@ntu.edu.tw

ABSTRACT

Tin monosulfide (SnS), an affordable group IV-VI compound, has emerged as a promising material due to its low toxicity, abundance, and potential for future semiconductor devices. The exceptionally low thermal conductivity from the strong lattice anharmonicity makes this material suitable for thermoelectric applications[1]. In general, the polycrystalline thermoelectric properties tend to show poor quality compared to its single-crystal counterpart[2]. Furthermore, the anisotropic performance based on the sintering process complicates the polycrystalline preparation of this material[3]. In this study, we successfully improved the electronic transport properties of polycrystalline SnS by utilizing the in-plane transport properties with texture modulation. It was found that the anisotropic transport properties were not only from the preferred orientation of the crystallite grain due to sintering but also from the strain of the out-of-plane SnS crystal, which led to enhanced in-plane electrical conductivity. Here, the enhancement of transport properties, by employing the lateral crystal structure, realized the highest reported electrical conductivity of polycrystalline SnS. Additionally, the hole carrier concentration of p-type SnS was further optimized by co-doping of silver and sodium. With these improvements, our co-doped SnS exhibits a relatively high power factor (PF) peak of ~4.49 μW cm^{-1} K^{-2} at 473 K and a high thermoelectric figure of merit, zT, ~0.3 at 573 K, making it promising for low-temperature applications involving sulfur-based polycrystalline thermoelectric materials.

References

1. Wu, H. et al. **Sodium-doped Tin Sulfide Single Crystal: A Nontoxic Earth‐Abundant Material with High Thermoelectric Performance**. Adv. Energy Mater. 8, 1‐8 (2018).
2. Zhou, B. et al. **Thermoelectric properties of SnS with Na-doping**. ACS Appl. Mater. Interfaces 9, 34033–34041 (2017).
3. Asfandiyar et al. **Thermoelectric SnS and SnS-SnSe solid solutions prepared by mechanical alloying and spark plasma sintering: Anisotropic thermoelectric properties**. Sci. Rep. 7, 1–7 (2017).

Study of Optical Chirality in Quasi-2D Chiral Perovskite Thin Films by Helicity-Resolved PL Spectroscopy

Ping-Shen Chang[1], Lan-Sheng Yang[1], Yu-Chiang Chao[1] and Ting-Hua Lu[1*]

[1]Department of Physics, National Taiwan Normal University, Taipei, Taiwan

E-mail: 41041221s@gapps.ntnu.edu.tw

ABSTRACT

Chiral materials in quasi-two-dimensional (quasi-2D) Ruddlesden−Popper (RP) perovskites are suitable for fabricating a wide range of devices, including spintronic and optoelectronic applications, due to their flexible crystal structure[1,2,3]. The integration of chiral organic ligands with RP perovskites imparts strong chirality, and the properties of visible photoluminescence (PL) can also be examined using the spin-angular momentum of excitation light[1,3]. Here, we have studied the helicity-dependent PL of quasi-2D chiral perovskite (R-/S-MBA)$_2$(MA)$_{n-1}$Pb$_n$I$_{3n+1}$ (MBA=$C_6H_5C_2H_4NH_3$, MA=$CH_3NH_3^+$) thin-films at room temperature by calculating the degree of circular polarization (DoCP) value. We observed that in both samples, the intensity of the PL from the helicity-exchanged portion is greater than that from the helicity-preserved portion. We further calculated that the average DoCP value is 4.22% for (R-MBA)$_2$(MA)$_{n-1}$Pb$_n$I$_{3n+1}$ under right-handed circularly polarized excitation light, while it is 5.07% for (S-MBA)$_2$(MA)$_{n-1}$Pb$_n$I$_{3n+1}$ under left-handed circularly polarized excitation light. The additional X-ray diffraction (XRD) and circular dichroism (CD) measurements offer a more comprehensive understanding of the chiral properties of the perovskites. The results show that utilizing helicity-dependent PL measurements gives the chiral material great potential for developing spin-associated electronic devices.

References

1. Jiaqi Ma, Chen Fang, Chao Chen, Long Jin, Jiaqi Wang, Shuai Wang, Jiang Tang, and Dehui Li, **ACS Nano**,13(3), 3659-3665(2019)
2. M. Rahil, R. M. Ansari, C. Prakash, S. S. Islam, A. Dixit, and S. Ahmad, **Scientific Reports**, 12(1), 2176 (2022)
3. Sile Hu, Bing Tang, Stephen V. Kershaw, Nicholas A. Kotov, and Rogach Andrey, **ACS Applied Materials & Interfaces**,16(10), 12965-12973(2024)

Theoretical Study of Passivation on Sn Perovskite Surface by Amine-based Molecules

Ryota Araki, Makito Takagi, Tomomi Shimazaki
Materials System Science Major, Graduate school of Nanobioscience,
Yokohama City University
e-mail: n245203a@yokohama-cu.ac.jp

ABSTRACT

【Introduction】

Perovskite solar cells have recently attracted much attention as next-generation solar cells because of their low manufacturing cost and their rapidly improving power conversion efficiency (PCE). It has been reported that defects at the interface of them would cause the decreasing the PCE.[1] To avoid this, the passivation technique, coating organic molecules on the perovskite surface, is frequently employed.[2] In our previous study, based on the DFT calculation, we have reported that the mechanism of passivation for the Sn perovskite surface by ethylene diamine (EDA) would be explained by orbital-defect interactions.[3]

In this study, we investigated the passivation effect on the Pb-free Sn perovskite surface by not only EDA but also several amine molecules and compared them.

【Result and discussion】

In this study, as a model of Sn perovskite defect surface, vacancy of Sn atom (V_{Sn}) on $MASnI_3$ (001) surface was used. For this defect surface model, DFT calculations of passivation by several amine molecules were performed: calculation level are set to bellow, PBE+D3, $k = 5\times5\times1$, cutoff = 450 eV.

As an example, the structure and density of states (DOSs) before and after methylamine adsorption on Sn perovskite surface are shown in **Fig. 1**. Before molecule adsorption (**Fig. 1(a)**), the defect level exists in the band gap in the DOS, while after adsorption (passivation) (**Fig. 1(b)**), it removed from bandgap. Similar improvement trends were also observed for other amine molecules. Furthermore, by comparing these results, it is suggested that the interaction between the passivation molecule and the surface defect would be important for improving the defect level.

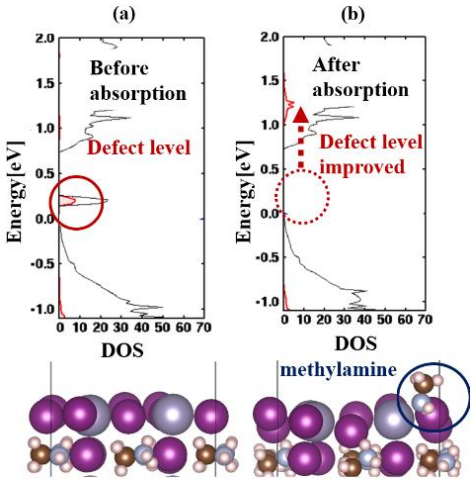

Fig .1 Structure and density of states (DOSs) before adsorption (a) and after adsorption of methylamine (b).

References

1. L. Bo, C. Bohong, P. Lu, L. Zihao, F. Lin, H. Zhubing, Y. Longwei, **ACS Energy Lett.**, *5*, 3752-3772, (2020).
2. X. Zewen, S. Zhaoning, Y. Yanfa, **Adv. Mater.**, *31*, 1803792, (2019).
3. N. Takumi, T. Makito, T. Masanori, Y. Koichi, and S. Tomomi, **J. Phys. Chem. Lett.**, *14*, 6695–6701, (2023).

Unveiling Local Activity in Layered TMDCs for Energy Conversion: A Combined SECM-AFM Approach

Sumangaladevi Koodathil[1,2,3,4], Septia Kholimatussadiah[4,5], Mohammad Qorbani[4], Raman Sankar[6], Li-Chyong Chen[4,5], Kuei-Hsien Chen[3,4].

1. Molecular Science and Technology Program, Taiwan International Graduate Program, Academia Sinica, Taipei 10617, Taiwan
2. International Graduate Program of Molecular Science and Technology, National Taiwan University, Taipei 10617, Taiwan
3. Institute of Atomic and Molecular Sciences, Academia Sinica, Taipei 10617, Taiwan
4. Center for Condensed Matter Sciences, National Taiwan University, Taipei 10617, Taiwan
5. Department of Physics, National Taiwan University, Taipei, Taiwan
6. Institute of Physics, Academia Sinica, Taipei,

e-mail: suma.parappa@gmail.com, d10551010@ntu.edu.tw

ABSTRACT

Transition metal dichalcogenides (TMDCs) hold promise as cost-effective electrocatalysts for renewable energy technologies. This study explores the crucial role of interfacial electron transfer in optimizing their performance. We employ scanning electrochemical microscopy (SECM) coupled with atomic force microscopy (AFM) to map the local activity of mechanically exfoliated 2D TMDCs. Our approach unveils layer-dependent activity and potential strain effects through SECM mapping. Additionally, we visualize layer-dependent surface potential variations using KPFM. This combined approach provides valuable insights into factors governing electrocatalytic performance in TMDCs, paving the way for the design of high-efficiency TMDC-based energy conversion systems.

References

1. Du, H. Y. et al. Nanoscale redox mapping at the MoS2-liquid interface. Nat. Commun. 12 (2021).
2. Qorbani, M. et al Atomistic insights into highly active reconstructed edges of monolayer 2H-WSe2 photocatalyst Nat. Commun volume 13, Article number: 1256 (2022)
3. Takahashi, Y. et al. Angew. Chem. Int. Ed. , 59, 3601 – 3608 (2020)

Preparation of SERS substrates by DC sputtering and annealing

Wataru Nakajima, Ryo Suzuki, and Masaru Tachibana
Graduate school of Nanobioscience, Yokohama City University, Japan
e-mail: n245216g@yokohama-cu.ac.jp

ABSTRACT

Raman scattered light has a different wavelength from that of the incident light, which is generated when a material is exposed to light. The attempt to analyze the characteristics of a material by examining this scattered light is called Raman spectroscopy. Raman spectroscopy is one of the powerful tools to evaluate various materials with non-contact and non-destructive measurements. However, Raman peak may not be often observed because the intensity is very weak depending on the sample. Therefore, a phenomenon called Surface-Enhanced Raman Scattering (SERS) is useful.

SERS is an enhancement of Raman spectroscopy. When metallic nanoparticles are exposed to excitation light, collective oscillations of electrons (localized plasmons) are generated. This localized plasmon creates an enhancement field around the metal particles.

In this study, we worked on the fabrication of SERS substrates. Au was sputtered onto a SiO_2 substrate via a sputtering apparatus. The UV spectra of the substrate were measured to investigate whether enhancement occurred. Fig.1 shows the UV spectra with and without annealing. As seen in the Fig.1, the distinctive absorption was not observed for the as-fabricated substrate. Then, an annealing with 300ºC for 2 hours was conducted based on the previous study [1]. As a result, the absorption at 541 nm wavelength was clearly observed. By annealing, Au layer was transformed into nanoparticles with spherical shape as shown in Fig.2. Therefore, the Raman spectra are expected to be enhanced.

In the presentation, the fabrication condition of substrates and the application for SERS will be discussed as well.

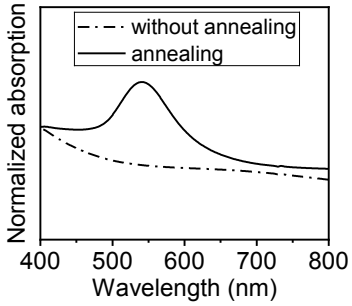

Fig.1 Comparison of UV spectra before and after annealing 300ºC

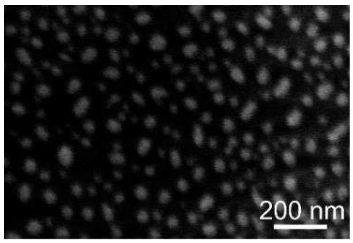

Fig.2 SEM image of sputtering time of 0.5 min and annealing at 500°C for two hours

References

[1] Thi Huyen Trang Nguyen *et al*.,**Optical Materials**. *121*, 111488-(2021).

Behavior of iron deposition on the surface structure and electrical properties of $CrBr_3$ by scanning tunneling microscopy and spectroscopy

<u>Yu Chieh Lo,</u> Bu Wei Huang, Yuan Ju Chang, Tsu Yi Fu

Department of Physics, National Taiwan Normal University, Taipei, 116059, Taiwan, ROC

e-mail: abcde30701889@gmail.com

ABSTRACT

In this study, we find that iron deposition caused significant changes to the energy band gap of Chromium Tribromide ($CrBr_3$), which decreased abruptly from 1.837 ± 0.058 eV to 0.148 ± 0.024 eV, indicating that a transition from a p-type semiconductor to semi-metal occurred. $CrBr_3$ is a well-known material due to its magnetic properties. There is a possible solution to overcome the limitation of low Curie temperature of $CrBr_3$ is to introduce a heterostructure by incorporating metallic elements. Therefore, we fabricate the $CrBr_3$/HOPG heterostructure by mechanical exfoliation and dry transfer techniques, and we conduct the deposition of iron atoms onto the surface of the heterostructure based on earlier finding. Our research supports the simulation of density functional theory in describing the electrical properties of $CrBr_3$ in previous research.

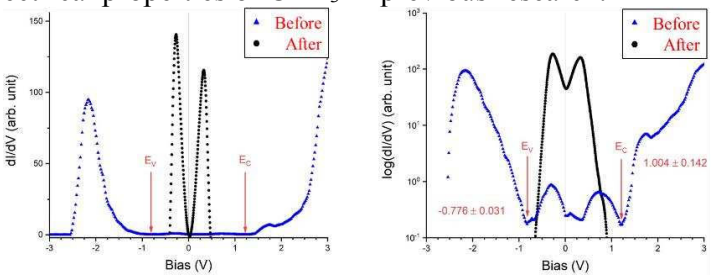

References

1. B. W. Huang, Y. J. Chang, Y. C. Lo, T. Y. Fu. Behavior of iron deposition on the surface structure and electrical properties of CrBr3 by scanning tunneling microscopy and spectroscopy. **Thin Solid Films**, *Volume 800*, 140409(2024).
2. X. F. Chen, Q. Yang, X. H. Hu. Tunable electronic and magnetic properties of transition-metal atoms doped CrBr3 monolayer. **Acta Phys. Sin.**, *70(24)*: 247401(2021).
3. Y. Wu, M. Zhu, R. Zhao, X. Liu, J. Shen et al.. Degradation Effect and Magnetoelectric Transport Properties in CrBr3 Devices. **Materials**, *15(9)*, 3007(2022).
4. Dinesh Baral, et al. Small energy gap revealed in CrBr3 by scanning tunneling spectroscopy. **Phys. Chem. Chem. Phys.**, *23*, 3225(2021).

Structural determination of fructooligosaccharides in onions using logically derived sequence tandem mass spectrometry

Wun-Long Li[1,2], Chi-Kung Ni[2,3]

[1] Institute of Atomic and Molecular Sciences, Academia Sinica, Taiwan

[2] Department of Chemistry, National Taiwan Normal University, Taipei, Taiwan

[3]Department of Chemistry, National Tsing Hua University, Hsinchu, Taiwan

e-mail: wsolee23@gmail.com

ABSTRACT

Fructooligosaccharides (FOS) are fructose-based oligosaccharides found in various flowering plant species. These oligosaccharides primarily serve as reserve carbohydrates and play crucial roles in plant disease resistance, cold and drought tolerance, and seed germination. FOS also provide several benefits to human health, such as immune system stimulation, proliferation of probiotic bacteria, and improvement of digestive health. Currently, the structural identification of FOS is primarily conducted using High-Performance Anion-Exchange Chromatography with Pulsed Amperometric Detection (HPAEC-PAD) for rapid analysis. This method relies heavily on comparison with standards. We now utilize a novel liquid chromatography-tandem mass spectrometry (LC-MS) method, called logically derived sequence tandem mass spectrometry (LDOES), capable of identifying carbohydrate structures with minimal sample amounts

References

1. Verspreeta, J.; Hansen, A. H.; Harrison, S. J.; Vergauwen, R.; Van den Ende, W.; Courtin, C. M. Building a fructan LC–MS2 library and its application to reveal the fine structure of cereal grain fructans. **Carbohyd. Polym**. *174*, 343–351 (2017).
2. Tsai, S.T., et al. Automatic full glycan structural determination through logically derived sequence tandem mass spectrometry. **ChemBioChem** *20*, 2351−2359 (2019)

Gate-Driven Photoluminescence Modulation of Monolayer MoS_2 FET

Yi-Chih Cheng[1,2], Cheng-Yu Huang[1,2], Jung-Chen Tung[1*], and Ting-Hua Lu[2*]

[1] Department of Electro-Optical Engineering, National Taipei University of Technology

[2] Department of Physics, National Taiwan Normal University, Taipei, Taiwan

e-mail: jerryspeed816@gmail.com

ABSTRACT

The tunable band gap in monolayer MoS_2 has advanced the development of field-effect transistors (FETs) that demonstrate excellent optical and electrical properties and reduced power dissipation, owing to their nanoscale thin-film flexible structure. The spin-orbit splitting in the band structure of MoS_2 leads to generating A and B exciton direct band gap transitions at the K and K' valleys, leading to the observation of strong photoluminescence. However, controlling the carrier density in MoS_2 FET devices is a highly effective method for modulating the photoluminescence (PL) properties of monolayer MoS_2[1,2,3]. In this study, we systematically varied the gate voltage and laser illumination power to observe the modulation of PL emission characteristics. We found that as the gate voltage increases from -40V to 40V, the A exciton intensity gradually decreases due to the interaction between excitons and carriers. We observed that the B exciton remains unaffected by gate voltage modulation. Additionally, we utilized different laser illumination powers to identify the trend where the A exciton exhibits the most significant changes. The results indicate that gate-driven PL modulation could be promising for advancing applications in valleytronics.

References

1. Y. Liu, T. Shen, S. Linghu, R. Zhu and F. Gu, **Nanoscale Advances**, *4.11*, 2484-2493 (2022).
2. X. Zhang, H. Nan, S. Xiao, X. Wan, Z. Ni, X. Gu and K. Ostrikov, **ACS Publications**, *9.48*, 42121-42130 (2017).
3. A.K.M. Newaz, D. Prasai, J.I. Ziegler, D. Caudel, S. Robinson, R.F. Haglund Jr. and K.I. Bolotin, **ScienceDirect**, *155*, 49-52 (2013).